The evolution of the North Atlantic AMOC since 1980

Laura C. Jackson[1,†], Arne Biastoch[2,3], Martha W. Buckley[4], Damien G. Desbruyères[5], Eleanor Frajka-Williams[6], Ben Moat[6], and Jon Robson[7]

[1]Met Office, Hadley Centre, Exeter, UK
[2]GEOMAR Helmholtz Centre for Ocean Research Kiel, Kiel, Germany
[3]Kiel University, Kiel, Germany
[4]Atmospheric, Oceanic and Earth Sciences, George Mason University, Fairfax, VA, US
[5]Ifremer, University of Brest, CNRS, IRD, Laboratoire d'Océanographie Physique et Spatiale, Plouzané, France
[6]National Oceanography Centre, Southampton, UK
[7]National Centre for Atmospheric Science, Department of Meteorology, University of Reading, Reading, UK
[†]e-mail: laura.jackson@metoffice.gov.uk

ABSTRACT

The Atlantic Meridional Overturning Circulation (AMOC) is a key component of the climate through its transport of heat in the North Atlantic. Decadal changes in the AMOC, whether through internal variability or anthropogenically forced weakening, therefore have wide-ranging impacts. In this Review, we synthesise understanding of contemporary decadal variability in the AMOC, bringing together evidence from observations, ocean reanalyses, forced models and AMOC proxies. Since 1980, there is evidence for periods of strengthening and weakening, although magnitudes of change (5-25%) are uncertain. In the subpolar North Atlantic, the AMOC strengthened until the mid-1990s and weakened until the early 2010s, with some evidence of a strengthening thereafter; these changes are likely linked to North Atlantic Oscillation-related buoyancy forcing. In the subtropics, there is some evidence of the AMOC strengthening from 2001-2005 and strong evidence of a weakening from 2005-2014. Such large interannual and decadal variability complicates detection of ongoing long-term trends, but does not preclude a weakening associated with anthropogenic warming. Research priorities include developing robust and sustainable solutions for the long-term monitoring of the AMOC; observation-modelling collaborations to improve the representation of processes in the North Atlantic; and better distinguishing anthropogenic weakening from internal variability.

Introduction

The Atlantic Meridional Overturning Circulation (AMOC; Box 1) is a system of ocean currents in the Atlantic that move warmer, upper waters northwards and cooler, deeper waters southwards. Accordingly, the AMOC is a major source of northward heat transport, accounting for 20-30% of total atmospheric and oceanic heat transport into the mid-latitudes[1]. The AMOC, therefore, has a key role in governing the climate of the North Atlantic region and beyond, influencing European air temperatures and precipitation, the frequency of Atlantic hurricanes and winter storms, spatial patterns of sea level and tropical monsoons[2,3], and the global carbon budget[4].

The strength of the AMOC is typically ~17 Sv (Sv=Sverdrup; 1 Sv = 10^6 m^3s^{-1})[5]. However, both observations and models indicate that the AMOC exhibits substantial variability on daily to multi-decadal timescales. Coupled climate models suggest decadal variability can arise naturally due to internal interactions within the climate system[6–8]. The AMOC is also expected to respond to external forcing, including anthropogenic aerosols, volcanic eruptions and solar changes[9,10], as well as anthropogenic greenhouse gas emissions[11]. Indeed, observations, reanalyses, models and proxies[12–16] indicate substantial contemporary decadal-scale changes in AMOC strength. The RAPID array at 26.5^{o}N[5,17], for example, revealed a statistically significant weakening from 2004 (ref[18,19]), likely representing decadal variability rather than ongoing long-term weakening[20–22]. There are indications that the AMOC might be recovering in strength[12].

Despite evidence of decadal variability, many questions remain. For example, high-quality continuous observations, like the RAPID array, are short and sparse, making it difficult to assess longer-term AMOC variability and determine whether decadal changes are representative of those across the wider Atlantic. Moreover, there is uncertainty about the relative roles of internal variability and forced variability, owing to diverse AMOC variability[8,23] and externally-forced AMOC trends[10,24] in models. Indeed, the AMOC might have already weakened over the 20th Century[25,26], potentially implying that it is more sensitive to external forcing than previously thought. Understanding how and why the AMOC has changed on decadal timescales is thus crucial to not only understand the AMOC's role in shaping the climate of the North Atlantic relative to other influences[27,28], but also to constrain predictions of future changes and AMOC impacts[2,29].

In this Review, we bring together and critically assess multiple lines of evidence to understand decadal-scale changes

in the AMOC since 1980, the time period selected owing to greater data availability. Given that decadal-scale variability likely has a larger impact on ocean temperatures than variability at shorter timescales[28], we focus discussion on multiannual and decadal timescales. We begin by reviewing current knowledge about the mechanisms driving AMOC variability and the methods and tools available to estimate it. We then outline and compare estimates of AMOC variability from the subtropical and subpolar North Atlantic regions, including indirect evidence from observed changes in the North Atlantic Ocean. We follow by discussing these changes in a longer term context, before ending with recommendations for future research.

AMOC variability

The AMOC exhibits substantial variability on intra-annual and seasonal timescales[30] (order 100% of its mean value) and much smaller variability on interannual to decadal timescales[7,30] (order 10-30%). Mechanisms of interannual-decadal AMOC variability depend strongly on the region of interest. In the subtropics, high-frequency (sub-annual to interannual) wind forcing dominates AMOC variability, with buoyancy forcing also contributing at low frequencies[28,31] (Fig 1). In contrast, low frequency variability (interannual to decadal) dominates the subpolar AMOC, with both wind and buoyancy forcing considered important[32–35]. The AMOC responds strongly to the North Atlantic Oscillation (NAO), the dominant mode of atmospheric variability in the North Atlantic, which leads to both wind-induced and buoyancy-induced AMOC variations[28]. The mechanisms driving AMOC variability are now discussed.

Wind forcing

Wind stress forcing creates AMOC anomalies through two mechanisms: Ekman transports and wind-induced geostrophic currents. Wind stress anomalies drive surface currents (Ekman transports) perpendicular to the wind, so zonal wind stress anomalies create meridional currents. To conserve mass, these Ekman transports must be balanced by a return flow in the opposite direction, creating a meridional overturning[36]. Spatial variations in Ekman transports also cause convergence and divergence, leading to downwelling and upwelling, respectively. These vertical velocities move the thermocline up or down (heaving), generating density anomalies and, thus, wind-induced geostrophic currents.

While the AMOC responds locally and instantaneously to wind-forcing through Ekman transports and heaving, the ocean also has slow and remote responses. Wind-induced thermocline variations propagate westward as baroclinic Rossby waves and can lead to western boundary density, and hence AMOC, anomalies in both subtropical[37,38] and subpolar latitudes[39]. The time taken for these waves to propagate varies from about a year in the subtropics to many decades in subpolar regions.

Wind-driven variations of the AMOC depend on the local winds, and so variability can differ by latitude[40–43]. However, given that a large portion of wind-driven variability results from the NAO, spatially coherent NAO-driven AMOC changes are often observed. Specifically, a positive NAO results in anomalous westerly winds over the subpolar North Atlantic and easterly winds over the subtropical North Atlantic (and vice versa for a negative NAO), driving AMOC variability of opposite sign between the subtropical and subpolar regions[44].

Buoyancy forcing

Buoyancy forcing (changes in surface density through surface heat and freshwater fluxes) results in water mass transformation[45,46] and densification of waters in the subpolar North Atlantic. The densest waters are formed in the Labrador Sea and the Nordic seas, with the reduction in stratification preconditioning deep convection. Model experiments suggest that large, decadal-scale AMOC variability in the North Atlantic primarily arises from bouyancy fluxes over subpolar regions associated with low frequency NAO variability[33,47–50]. In particular, a positive NAO results in stronger winds over the subpolar North Atlantic and, hence, increased heat loss to the atmosphere and greater dense water formation; a negative NAO has the opposite effect. Numerous model simulations indicate that anomalies of deep convection and subsurface density anomalies in the subpolar North Atlantic precede AMOC anomalies[6,51–54].

However, understanding of the connections between overturning, water mass formation and convection are thought to be incomplete. For example, observations have been unable to show direct links between Labrador Sea Water formation[55–58] and AMOC variability[59]. Instead, changes in Labrador Sea Water formation rates might only change the volume or density of Labrador Sea Water within the subpolar North Atlantic rather than its export[60,61]. However, longer time averages (decade or longer) might be required to see a direct correspondence between formation rates and export[12,62,63]. Moreover, observations suggest that AMOC mean strength and sub-annual variability are dominated by variations east of Greenland[12,64–66], whereas models frequently highlight the Labrador Sea as a key region for deep water formation and originator of AMOC variability[23,50,67]. Yet, some coupled models do show agreement with observations[68–70] and suggest AMOC variability can be dominated by the eastern subpolar region while still having strong correlations between the AMOC and Labrador Sea properties[69]. The interpretation of model results might therefore be flawed rather than the models themselves.

Oceanic processes and AMOC feedbacks

AMOC anomalies can be generated by purely oceanographic processes. For example, baroclinic instability can spontaneously generate ocean eddies, adding chaotic-intrinsic variability to the AMOC[71–73], as well as force baroclinic Rossby waves[39,72,74–76]. Both eddies and Rossby waves modify the east-west density difference, thus contributing to AMOC anomalies[37,75].

AMOC variability can also involve ocean or coupled feedbacks that amplify (positive feedback) or dampen (negative feedback) the initial perturbation. For example, AMOC-related heat and freshwater transport changes can modify advection and thus subpolar density, in turn impacting the AMOC[51,77–79]. AMOC-driven SST anomalies can also change atmospheric circulation, perturbing the NAO[80–82]. However, the importance of both these processes in explaining decadal AMOC variability is unclear. For instance, coupled models simulate a range of advective feedbacks with differing roles for heat and freshwater transports[51,77–79,83], and the atmospheric response to AMOC-related SST anomalies is often weak and inconsistent across models[84,85].

Southward communication of AMOC anomalies

While many AMOC anomalies remain localized, some are communicated meridionally to give rise to large-scale AMOC variations. Large-scale AMOC anomalies are thought to be generated in the subpolar gyre and communicated southward into the subtropical gyre[32,86] either slowly through advection of deep subpolar density anomalies[87], or more quickly through boundary waves[86,88,89]. There is strong mixing of these dense waters before reaching the subtropics[90–92], meaning only large and persistent AMOC anomalies might succeed in being communicated southward[93,94].

Measuring and modelling the AMOC

As the AMOC varies on different timescales, it is important to have continual measurements of its strength. Estimates come from direct observations, models, reanalyses and proxy records, and when used together, can improve the understanding of the robustness of signals.

Observations

Historically, measurements of AMOC strength come from longitude-depth temperature and salinity measurements at particular times; these measurements are converted to AMOC strength by applying the thermal wind relationship (which relates zonal density gradients with vertical gradients in meridional velocity)[95], sometimes using box inverse models[22]. While such AMOC estimates provide key benchmarks for validating time series obtained from time-continuous measurements[96], they suffer from aliasing of large monthly and interannual variability, and are likely inadequate to examine decadal changes in ocean transport[97].

The RAPID/MOCHA/WBTS 26.5^{o}N array[5,98](Box 1) has measured AMOC variability since 2004, delivering an in-depth view of its circulation[17]. The array consists of moorings near the Bahamas and Canary Islands which make continuous measurements of temperature and salinity to compute relative velocities in the interior ocean. AMOC strength is calculated from the full velocities, requiring the addition of a reference level velocity (obtained by setting the total volume transport through the section), and combining with near-surface Ekman transport from wind stress in atmospheric reanalyses and Gulf Stream transport from a submarine cable[5]. The OSNAP (Observing the subpolar North Atlantic program) array started in 2014 (ref[65]), although is not yet long enough to examine interannual or decadal variability. While mooring-derived calculations (such as RAPID[98]) are the most valuable method for measuring the AMOC, they still suffer from data gaps (in particular surface layers and continental slopes) and from difficulty in robustly determining the reference velocity.

Other observation-based methodologies complement these arrays and extend AMOC estimates back in time or to other latitudes. The most common methodology uses alternative data sets (shipboard hydrographic sections or Argo profiling floats[99]) to generate gridded fields of temperature and salinity at monthly resolutions from which relative velocities can be computed. These relative velocities are then combined with a reference level velocity (obtained from satellite-based measurements of surface currents or directly estimated from float displacements near 1000m depth) and Ekman wind stress using atmospheric reanalyses[12,96,100]. Arrays using such methods, including at A25-OVIDE[96], 41^{o}N[100] and 45^{o}N[12], have additional uncertainties owing to irregular and limited data distribution, notably along basin margins where strong and narrow boundary currents are insufficiently sampled.

At 26.5^{o}N, an additional reconstruction has extended the AMOC timeseries using Gulf Stream cable measurements and sea-level anomalies measured by satellite altimetry[101], with an updated reconstruction taking into account the vertical structure[102]. Building on a clear relationship between western boundary sea-level anomalies and upper mid-ocean geostrophic transport changes, these reconstructions recover a large fraction of the directly-observed AMOC interannual variability[101]. Although these methodologies provide key multi-decadal records, they rely on a fragile linear and time-invariant relationship between sea-level anomalies and interior density changes.

An alternative methodology relies on a balance between the northward import of light waters, their densification through air-sea buoyancy fluxes, and their southward export as dense waters[45,103,104]. Accordingly, it becomes possible to reconstruct

an AMOC time series from surface observations alone[12]. This estimate is expected to lead AMOC variability observed downstream of water mass transformation sites by several years owing to the time of advection of buoyancy anomalies by the mean circulation. While providing an independent measure of the AMOC, such relationships between transformation and the AMOC might only hold on longer (decadal) timescales and neglect diapycnal mixing.

Models and reanalyses

AMOC changes can also be assessed using numerical models, either with forced ocean models[105,106] (ocean models forced with historical atmospheric conditions) or ocean reanalyses[107] (forced ocean models that assimilate observations). Models and reanalyses provide more complete, physically consistent views of the ocean, both spatially and temporally. However, both rely on imperfect ocean models; insufficient resolution often incorrectly simulates processes such as eddies, convection and overflows[108], resulting in different AMOC strength compared to eddy-rich models[109,110]. Ensembles of forced ocean models[14,111] are generally able to reproduce the mean structure of the AMOC[68,110,111] and interannual variability, given that interannual variability is mainly wind-driven and the forcing sets are well-constrained by satellite winds[112,113]. However, AMOC trends and decadal variability can be affected by uncertainties in surface fluxes and the different methods used to impose and correct them[112,114,115].

Ocean reanalyses are ocean models further constrained by observations such as SST, sea ice concentration and sea surface height from satellites, and subsurface observations of temperature and salinity. These constraints potentially have the advantage of providing a more observationally-consistent estimate of the AMOC, but the assimilation itself can generate spurious effects. Reanalyses vary substantially with different data assimilation strategies (from nudging to adjoint methods[107]) and the observations that are assimilated. In particular, there has been a large increase in available observations from satellite measurements (since the early 1990s) and Argo profiling floats[116] (since the early 2000s). Reanalyses focusing on earlier periods have little agreement in AMOC variability[112,117]. However, the agreement is much stronger since the mid 90s, particularly for reanalyses, which use the wide variety of observational constraints available since 1993 (ref[13]).

Coupled models are simulations of the oceans and atmosphere, where instead of applying historical atmospheric conditions to force the ocean, both the ocean and atmosphere are free to evolve and interact. They are important tools for understanding the spectrum and mechanisms of AMOC variability on a range of timescales. However, as AMOC variability is not constrained by atmospheric fluxes and observed ocean properties, coupled models are not expected to represent the observed internal variability of specific time periods. Nevertheless, they can be used to examine the forced response of the AMOC to historical greenhouse gas and aerosol changes.

Indirect evidence

In addition to observations, models and reanalyses, estimates of the AMOC can be determined by considering changes in the North Atlantic Ocean that are mechanistically and statistically associated with the AMOC[118,119]. Such proxies can be used to reconstruct AMOC timeseries, and are often developed using relationships derived from models owing to limited direct observations. An understanding of the robustness of these relationships is needed. For example, because models indicate causal relationships between the AMOC and North Atlantic ocean temperatures, and because there are long records of upper ocean temperatures, proxies based on SSTs and subsurface temperatures have been proposed[120–123]. These relationships occur because changes in the AMOC affect ocean heat transport, which, in turn, affects the rate of change of heat content. Hence, an SST signal would be expected to lag the AMOC by a few years[7,122], though results are sensitive to the latitude of the AMOC index.

Other proxies have made use of relationships between the AMOC and subsurface density in the Labrador sea[15,124] and with sea level records along the eastern seaboard of North America[125,126]. Paleoclimate data potentially provides very long records. Although most cannot resolve decadal variability, sortable silt[127], a proxy for deep western boundary current speeds, has sufficient temporal resolution to estimate variability since the 1980s.

Changes in the AMOC

The multitude of AMOC observations, reconstructions and models offer opportunities to assess and compare contemporary AMOC changes for both the subpolar and the subtropical North Atlantic (Fig 2, 3), where variability and drivers can differ. AMOC variability since 1980 (when consistent records are available) is now discussed.

Subpolar AMOC

Since 1980, evidence suggests the subpolar AMOC strengthened to the mid-90s, weakened from the mid-90s to 2010s, with some indications for strengthening since 2010.

The initial strengthening from the 80s to the mid-90s is evident in several data sets. The forced ensemble[106], the only reconstruction extending back to 1980, reveals an AMOC strengthening of ~ 2 Sv (Fig 2e), consistent with that of an earlier

forced ensemble[112]. Proxy reconstructions of subpolar North Atlantic density[15,124], sortable silt[127] and sea level anomalies[125] further depict increases to the mid 1990s (Fig.3a-c). Although the sortable silt proxy is measured at 35^{o}N (in the subtropics), it represents the deep western boundary current speed and, thus potentially, the propagation of changes from the subpolar North Atlantic.

All reconstructions and the subpolar proxies subsequently suggest a weakening of the AMOC from the mid 1990s (Fig 2a-e and Fig.3a-c), in agreement with previous results[32,33,48]. For example, from 1993-2013, statistically significant trends (P<0.05) of -0.26 Sv/year, -0.15 Sv/year, -0.14 Sv/year, -0.06 Sv/year and -0.18 Sv/year are evident from AMOC estimates at 45^{o}N (in depth and density space), from surface fluxes, reanalyses and forced models, respectively. At OVIDE, however, the -0.13 Sv/year AMOC reduction is not statistically significant. Hence there is strong evidence for a weakening AMOC at subpolar latitudes following the mid 1990s, but the magnitude of this weakening remains uncertain. Although these reconstructions differ in whether the AMOC was computed in density or depth space, and whether the wind-driven Ekman component was included, such differences do not explain the range of trends found.

Long-term moorings of the western boundary current system at 53^{o}N also provide evidence of a $\sim$ 10% decline in deep water export since 1998 (ref[128,129]). Yet further north, the export of dense water across the Greenland-Scotland ridge has remained stable since the early 1990s[130]. Accordingly, the source of decadal variability originates south of the overflows but north of 45^{o}N[12], consistent with observations of dense anomalies and enhanced deep convection in the west subpolar North Atlantic (south of the overflows) in the mid-90s[15,57].

Following this mid-90s to early 2010s AMOC weakening, there have been some indications of potential strengthening[12]. In particular, there has been an increase in density and deep convection in the subpolar North Atlantic[15,57,58], and an increase in the AMOC from observational reconstructions (Fig 2a-c) and sub-polar density and sea level proxies (Fig.3a,c). However, this strengthening is not present in reanalyses or forced models (though both show a cessation of a weakening trend), and the magnitudes and timing of this strengthening vary across the different observational reconstructions and proxies.

These decadal changes in subpolar AMOC have been attributed to low-frequency atmospheric variability and associated buoyancy forcing[32,33,48,131]. In particular, persistent and intense positive winter NAO in the early 1990s, a subsequent weakening of the winter NAO index until $\sim$2010 and strengthening thereafter[132], are all broadly consistent with with observed AMOC variability. However, salinity changes are thought to also have contributed to subpolar AMOC changes. For example, there is evidence that a small long-term freshening trend contributed to the very low subsurface density anomalies observed in the Labrador Sea post-2000 (ref[15,133]), with suggestions that melting from Greenland ice sheets might have contributed[134]. Variability in Arctic export of fresh water has led to "great salinity anomalies" in the subpolar North Atlantic in the 70s, 80s and 90s, though the impact these salinities might have had on the AMOC is uncertain[135–137].

Subtropical AMOC

The subtropical AMOC exhibits different variability from that of the subpolar AMOC, with purported strengthening from 2001-2005 and weakening from 2005-2014. Although there is agreement between different reconstructions on interannual variability, there is uncertainty on changes over longer timescales.

The longest estimate for the subtropical AMOC is from the ensemble of forced models, which reveals an AMOC strengthening to around 1998 and weakening thereafter (Fig 2j). These features are also seen in other forced model ensembles[14,112], including eddy-rich models[109,110] (Supplementary Fig. 1), though no obvious influence of resolution on the response to forcing was found[109,110]. Although the weakening in the forced models is statistically significant from 1998-2018, it is not apparent in other subtropical AMOC reconstructions (Fig 2g,h,i), and is, thus, uncertain.

There is, however, agreement on multi-annual AMOC changes and the decadal AMOC weakening observed by the RAPID array. Over 1993-2015, all subtropical AMOC reconstructions (Fig 2g-j) are significantly correlated (P<0.05) (other than between the 41^{o}N reconstruction and the forced ensemble), leading to confidence in the estimates of variability. The observational reconstruction at 41^{o}N is close to the inter-gyre boundary between subtropical and subpolar regions[28]. Although this reconstruction has previously been assumed to be representative of the subpolar North Atlantic[138], the variability at 41^{o}N bears more resemblance to observational reconstructions in the subtropical North Atlantic (Fig 2h), suggesting that the inter-gyre boundary is north of 41^{o}N.

All reconstructions suggest a 0.21-0.69 Sv/year increase in subtropical AMOC strength from 2001-2006. However, these trends are only statistically significant for the AMOC reconstruction at 26.5^{o}N (Fig 2g) and the ensemble mean of the reanalyses (Fig 2i). All individual reanalyses also illustrate a strengthening over this period[13].

Following this strengthening, the RAPID array shows a weakening of 0.4 Sv/year from 2005-2014[18] (Fig. 2f). This decadal weakening is statistically significant even when neglecting the temporary 2009-2010 dip[18], and is consistent with decadal variability in climate models[21,139]. Other reconstructions similarly capture a decadal weakening at this time, although trends of the order 0.23-0.27 Sv/year are somewhat weaker. Since 2014 the AMOC has been steady, or slightly increasing, although this increase is not statistically significant[30].

There is uncertainty about the drivers of these changes. Most of the monthly and interannual variability can be attributed to wind forcing, including the negative NAO-related dip in 2009/10[113,140–142]. There is also evidence of a buoyancy forced contribution to the decadal weakening from 2005-2014 (ref[31,142]), in particular through warming and freshening of the deep waters (below 1200 m) at the western boundary[143]. Although these signals were found in waters associated with North Atlantic deep water (formed in the subpolar North Atlantic), there is no observational evidence of subpolar-to-subtropic signal propagation or consensus on how subpolar changes might have influenced subtropical AMOC variability. For example, the strong subtropical AMOC in 2004-2006 has been linked to the strong subpolar AMOC in the mid 1990s through decadal propagation of subpolar dense anomalies[20]. However, the strong subpolar AMOC in the mid 1990s has also been linked to a strong subtropical AMOC in the late 1990s, with a faster propagation time[30,112]. While some models also suggest meridional linkages of AMOC variability[86–88], the processes and timescales vary, and it might be that some subpolar signals do not reach the subtropics[90,91,93].

Impacts on heat and freshwater

AMOC variability can impact Atlantic Ocean heat and freshwater content. Hence, observations of temperature and salinity patterns can be used to infer AMOC changes if other contributions to heat and freshwater budgets are assumed to be small. Between the early-1990s and the mid-2000s, upper ocean temperature increased in the subpolar North Atlantic and in the tropics, but decreased along the Gulf Stream path (Fig 4). This pattern is consistent with Atlantic Multidecadal Variability (AMV)[3], which in models, is linked to an increase in the AMOC[51,78,80,125]. After 2007, these trends reversed, cooling the subpolar North Atlantic and warming the western subtropics[3,15,144,145](Fig 4). Since 2015, upper subpolar North Atlantic layers warmed by around 0.2-1^{o}C, with salinity also increasing[15,145] by 0.02-0.1 PSU (Fig 4). The similarity in temperature and salinity patterns provides evidence for changes in advection affecting both heat and freshwater transports. These temperature and salinity changes are consistent with subpolar AMOC variability: a strong AMOC in the mid 1990s (leading to greater heat and salt transports across 45/50^{o}N, hence warming and salinification of the subpolar North Atlantic and cooling and freshening of the subtropics), a weak AMOC around 2010 (leading to a reversal in the pattern), and a stronger AMOC since 2015.

Several proxies representing AMV[120,121], subpolar North Atlantic SSTs[123] and subpolar North Atlantic subsurface temperatures[146,147], also illustrate an AMOC increase from the mid-90s to the mid-2000s, followed by a decrease (Fig.3d-f). This variability is closer to that seen in the subtropical AMOC reconstructions than the subpolar reconstructions. However, ocean temperature changes can lag the AMOC by several years[147], and lags can differ across models[7,122] and depend on the latitude the AMOC is measured at[122]. Hence, there is some uncertainty as to which aspects of the AMOC these proxies represent.

Changes in temperature and salinity can be driven by a number of processes. Although some cooling in 2014 can be related to surface fluxes[148], observed heat budget reconstructions[12,16,48] suggest that temperature trends cannot be fully explained by variations in surface heat fluxes alone, and are rather due to the varying magnitude of ocean heat transport convergence resulting from changes in the AMOC and horizontal gyre circulations[144]. In particular, the 2007-2015 cooling (and freshening) of the subpolar North Atlantic results from weak heat (and salt) transports across 45^{o}N[145], consistent with the reduced strength of the AMOC at 45^{o}N[12]. Likewise, the latest cooling-to-warming reversal was likely driven by changes in ocean heat advection from the subtropics with a lesser (yet non-negligible) role of air-sea heat fluxes[149], consistent with a strengthening of the subpolar AMOC since 2010 (Fig. 2a-c).

While AMOC variability is an important driver of North Atlantic temperature and salinity, as suggested by models[3,87] and observations[150], uncertainties about its relative contribution exist. Indeed, other processes can also be important, including local atmospheric forcing[151,152] and external forcing[2,153]. Furthermore, coupled models tend to underestimate the magnitude of decadal SST variability in the North Atlantic compared to observations[154], so the dominant mechanisms of decadal SST variability might differ between models and observations.

Long term context

In addition to internal variability, the AMOC can also vary owing to external forcing such as changing greenhouse gas concentrations or aerosols (Fig 1). Externally-forced AMOC changes, historical evolution and future projections are now discussed.

Forced changes

Given that ensemble averaging cancels out internal variability leaving only an externally-forced response, ensemble means of climate models can be used to examine the impact of external forcing on the AMOC. Generally, increased greenhouse gases are expected to weaken the AMOC through warming-related reductions in subpolar density[155,156], exacerbated by freshening from increased precipitation, sea ice loss and ice sheet melting[157]. Anthropogenic aerosol increases also cause a strengthening of the AMOC in models. Differing mechanisms have been proposed to explain this connection, including cooling through modified

heat fluxes[158] and increases in salinity through changes in evaporation and precipitation[131,159]. In addition to this mechanistic uncertainty, historical anthropogenic forcing itself remains uncertain[160]. As such, the extent that aerosol forcing has driven historical AMOC changes remains an open question.

An ensemble mean of historical (1850–2014) CMIP6 simulations (Fig 5) reveals a 10% strengthening of the AMOC to a maximum around 1980, followed by a weakening (-1.2 $\pm$ 0.2 Sv over 2004–2014 minus 1974–1984)[24]. This AMOC strengthening is attributed to changes in anthropogenic aerosol concentrations, with a small overall weakening from increases in greenhouse gases[10]. However, there is evidence that CMIP6 models with the strongest aerosol forcing overestimate its impact[10,161], and hence uncertainty around the historical forced response. The forced weakening since 1980 from CMIP6 simulations (Fig 5) is not seen in estimates of subpolar or subtropical AMOC changes (Fig 2), but the small magnitude of this forced change in comparison to the decadal and interannual variability of the AMOC would make it difficult to detect.

Linking to the past

There are substantial uncertainties in how the AMOC might have changed over the past few centuries. In particular, while model ensembles indicate a 20th century strengthening, salinity[162] and sea level[163] proxies, along with palaeoclimate records[26,123,127,164], all indicate a weakening, albeit with variations in timing and magnitude. Proxy observations reveal a region of reduced warming (a "warming hole") developing over the last century in the subpolar North Atlantic that some model simulations suggest is related to a weakened AMOC and ocean heat transports. Indeed, a proxy for AMOC strength using the difference between warming hole SSTs and global mean SSTs[25,123] suggests a 3 $\pm$ 1 Sv AMOC weakening since the middle of the twentieth century. However, the interpretation of this proxy for AMOC changes[10,119,164,165] and its applicability to the historical period[10,165] have substantial uncertainties. Although it has been suggested that this weakening is the result of fresh water from melting glaciers[123] (which climate models represent poorly or not at all), such impacts are not yet considered large enough to influence the AMOC[166,167]. Apparent model-proxy conflicts over the historical AMOC record might arise from proxies being unable to capture AMOC variations, particularly in the presence of large changes in forcing over different periods, or because of model deficiencies in the response of the AMOC to forcing.

Future projections and predictions

To understand how the AMOC might evolve in the future, climate models must be used. Over the next century, a long term weakening of the AMOC is expected owing to increased greenhouse gases[11,24]. However, there is substantial uncertainty in the magnitude of this weakening arising from differences in how individual models respond to forcing[24,168,169]. Nevertheless, a relationship between the present-day AMOC strength and projected weakening in CMIP6 models provides an emergent constraint, suggesting a 6-8 Sv (34-45%) decrease in AMOC strength by 2100 (ref[24]). Differences in the mean climate state, in particular the locations of water mass transformation, can also affect AMOC projections. For example, in some models, a higher resolution ocean impacts the climate state and leads to a greater projected AMOC weakening[170], but different models have different responses[171].

In contrast to the longer-term weakening, AMOC variability over the next decade or two is likely to be caused by a mix of long-term forced decline and internal variability. On these timescales, the internal variability is of similar magnitude to the forced changes (Fig 5). Thus, internal AMOC variability could oppose or reinforce the long-term trend making it difficult to detect (Fig 5). There is potential for predictability using a multimodel mean[172]. For example, predictions made in 2020 using 7 near-term prediction systems suggest the AMOC will be weaker in 2021–2025 than the 1981–2010 average, but there is considerable uncertainty in these predictions[173] and weak skill in the subtropics[174]. Although a long-term AMOC weakening is considered very likely in the future, a temporary strengthening related to decadal variability is possible. Predicting the evolution of the AMOC over the next decade or so is, thus, a major goal.

Summary and future perspectives

Having critically assessed decadal AMOC variability since 1980, both models and observations indicate that the AMOC varies on interannual and decadal timescales, with differences between the subpolar and subtropical North Atlantic. For the subpolar AMOC, there is strong evidence for a buoyancy forced increase in AMOC strength from at least 1980 to the mid 1990s, a weakening over the following 20 years[15,32,33,48], and emerging evidence of strengthening at 45^{o}N since the early 2010s[12]; this latter strengthening is not yet apparent in all lines of evidence, and the relative magnitude of this strengthening varies substantially. In the subtropics, by contrast, there is some evidence of an AMOC strengthening from 2001-2005, strong evidence (including from direct measurement at the RAPID array) of a decadal AMOC weakening from around 2005, and relative stability since the early 2010s[18,30]. It is difficult to determine any coherence between AMOC variability in the subpolar and subtropical regions, specifically the propagation of signals from the former to the latter. Although a long-term weakening of AMOC has previously been suggested, there is no evidence for such changes in the subpolar or subtropical AMOC from 1980 to the present day, in agreement with modelling results[22,175]. However, a gradual long-term weakening could be obscured

by the large interannual and decadal variability. Hence, these changes are not inconsistent with a weakening over a much longer period, such as that expected from anthropogenic warming[11,24].

Despite understanding of decadal-scale AMOC changes, there are still many unknowns and challenges. For instance, existing observational mooring arrays are expensive and lack sustainable funding. Thus, low-cost approaches to AMOC monitoring are required, perhaps through reduced complexity arrays (for example with fewer instruments or moorings), with their accuracy being tested with numerical models. Such long-term monitoring is required at both subtropical and subpolar latitudes.

In addition to long-term observations, there is scope to develop alternative methods for monitoring the AMOC. Alternative approaches that make use of existing observations, such as observational reconstructions, proxies and reanalyses, should be further explored: data science techniques might provide new methodologies for combining observations. Given uncertainties in different monitoring strategies we recommend using multiple, independent estimates of the AMOC to increase confidence in results.

Climate and ocean models also offer opportunities to better understand the AMOC, and to provide predictions and projections of its future evolution. However, certain processes, such as mixing by mesoscale eddies, transports in narrow boundary currents, mixing in overflows, deep convection and atmosphere-ocean feedbacks are often inadequately represented[108]. These deficiencies can lead to model biases, impacting how the simulated AMOC evolves[170]. Therefore, understanding and constraining the causes of model error is an important route to improving AMOC simulations and predictions. It is also crucial to better understand the causal relationships between processes such as surface buoyancy forcing, deep convection, sinking and the AMOC, and whether these interactions are correctly represented in models[59,65,69]. Unravelling these causal relationships requires improved understanding from both detailed observations and high-resolution process studies, especially given that small scale processes are likely to be key. Long term measurements remain important in this regard[19,59,176,177], and increasing sampling in less observed regions of the North Atlantic, such as the deep ocean and in boundary currents, is vital[178]. Increasing the resolution might also be an important route for improving the representation of the AMOC in coupled models, but resolving all these processes will be difficult to achieve for the foreseeable future owing to the computational expense. Technical solutions to improve resolution where it is needed, such as nested models or unstructured grids, might be an alternative, though improved representations of unresolved processes will still likely be needed through improved parameterisations. Doing so requires collaborations across observational, process-modelling and climate modelling communities.

Finally, there needs to be better understanding of how to separate forced trends (from greenhouse gases and aerosols) and internal variability in order to detect weakening from anthropogenic climate change. One approach might be to to use large ensembles of simulations to quantify how individual drivers and variability imprint on the AMOC and wider ocean patterns, and to examine where they differ. Understanding how robust these patterns are in different models and scenarios might also help to reconcile historical changes implied by proxies and climate models[10,26,164,165]. Partial coupling or coupled data assimilation might close the gap between forced ocean models and climate models, offering the opportunity to understand historical AMOC drivers while still correctly representing coupled processes. Improvements to predict and quantify the AMOC evolution of the coming decades is a major goal and requires a better understanding of the processes and model improvements.

References

1. Trenberth, K. E., Zhang, Y., Fasullo, J. T. & Cheng, L. Observation-based estimates of global and basin ocean meridional heat transport time series. *J. Clim.* **32**, 4567–4583 (2019).

2. Bellomo, K., Angeloni, M., Corti, S. & von Hardenberg, J. Future climate change shaped by inter-model differences in atlantic meridional overturning circulation response. *Nat. Commun.* **12**, 3659, DOI: 10.1038/s41467-021-24015-w (2021).

3. Zhang, R. *et al.* A review of the role of the atlantic meridional overturning circulation in atlantic multidecadal variability and associated climate impacts. *Rev. Geophys.* **57**, 316– 375, DOI: 10.1029/2019RG000644 (2019).

4. Sarmiento, J. L. & Le Quere, C. Oceanic carbon dioxide uptake in a model of century-scale global warming. *Science* **274**, 1346–1350 (1996).

5. McCarthy, G. D. *et al.* Measuring the Atlantic meridional overturning circulation at 26°N. *Prog. Oceanogr.* **130**, 91–111, DOI: 10.1016/j.pocean.2014.10.006 (2015).

6. Danabasoglu, G. On multidecadal variability of the Atlantic Meridional Overturning Circulation in the Community Climate System Model Version 3. *J. Clim.* **21**, 5524–5544, DOI: 10.1175/2008JCLI2019.1 (2008).

7. Ba, J. *et al.* A multi-model comparison of Atlantic multidecadal variability. *Clim. Dyn.* **43**, 2333–2348, DOI: 10.1007/s00382-014-2056-1 (2014).

8. Wills, R. C., Armour, K. C., Battisti, D. S. & Hartmann, D. L. Ocean–atmosphere dynamical coupling fundamental to the atlantic multidecadal oscillation. *J. Clim.* **32**, 251–272 (2019).

9. Otterå, O. H., Bentsen, M., Drange, H. & Suo, L. External forcing as a metronome for atlantic multidecadal variability. *Nat. Geosci.* **3**, 688–694 (2010).

10. Menary, M. B. *et al.* Aerosol-forced amoc changes in cmip6 historical simulations. *Geophys. Res. Lett.* DOI: 10.1029/2020GL088166 (2020).

11. Collins, M. *et al.* Long-term Climate Change: Projections, Commitments and Irreversibility. In Stocker, T. F. *et al.* (eds.) *Climate Change 2013: The Physical Science Basis. Contribution of Working Group I to the Fifth Assessment Report of the Intergovernmental Panel on Climate Change*, DOI: 10.1017/CBO9781107415324.025 (Cambridge University Press, Cambridge, United Kingdom and New York, NY, USA., 2013).

12. Desbruyères, D., Mercier, H., Maze, G. & Daniault, N. Surface predictor of overturning circulation and heat content change in the subpolar north atlantic. *Ocean. Sci.* **15**, 809–817, DOI: 10.5194/os-15-809-2019 (2019).

13. Jackson, L. C. *et al.* The mean state and variability of the north atlantic circulation: A perspective from ocean reanalyses. *J. Geophys. Res. Ocean.* **124**, 9141–9170, DOI: https://doi.org/10.1029/2019JC015210 (2019).

14. Tsujino, H. *et al.* Evaluation of global ocean–sea-ice model simulations based on the experimental protocols of the Ocean Model Intercomparison Project phase 2 (OMIP-2). *Geosci. Model. Dev. Discuss.* **2020**, 1–86, DOI: 10.5194/gmd-2019-363 (2020).

15. Robson, J., Ortega, P. & Sutton, R. A reversal of climatic trends in the North Atlantic since 2005. *Nat. Geosci.* **9**, 513–517, DOI: 10.1038/ngeo2727 (2016).

16. Bryden, H. L. *et al.* Reduction in ocean heat transport at 26°n since 2008 cools the eastern subpolar gyre of the North Atlantic ocean. *J. Clim.* **33**, 1677–1689, DOI: 10.1175/JCLI-D-19-0323.1 (2020).

17. Srokosz, M. A. & Bryden, H. L. Observing the Atlantic meridional overturning circulation yields a decade of inevitable surprises. *Science* **348**, 1255575, DOI: 10.1126/science.1255575 (2015).

18. Smeed, D. A. *et al.* Observed decline of the Atlantic meridional overturning circulation 2004-2012. *Ocean. Sci.* **10**, 29–38, DOI: 10.5194/os-10-29-2014 (2014).

19. Smeed, D. A. *et al.* The North Atlantic Ocean Is in a State of Reduced Overturning. *Geophys. Res. Lett.* **45**, 2017GL076350+, DOI: 10.1002/2017gl076350 (2018).

20. Jackson, L. C., Peterson, K. A., Roberts, C. D. & Wood, R. A. Recent slowing of Atlantic overturning circulation as a recovery from earlier strengthening. *Nat. Geosci* **9**, 518–522, DOI: 10.1038/ngeo2715 (2016).

21. Latif, M., Park, T. & Park, W. Decadal atlantic meridional overturning circulation slowing events in a climate model. *Clim. Dyn.* **53**, 1111–1124, DOI: 10.1007/s00382-019-04772-7 (2019).

22. Fu, Y., Li, F., Karstensen, J. & Wang, C. A stable atlantic meridional overturning circulation in a changing north atlantic ocean since the 1990s. *Sci. Adv.* **6**, eabc7836, DOI: 10.1126/sciadv.abc7836 (2020).

23. Danabasoglu, G., Landrum, L., Yeager, S. G. & Gent, P. R. Robust and nonrobust aspects of Atlantic Meridional Overturning Circulation variability and mechanisms in the Community Earth System Model. *J. Clim.* **32**, 7349–7368, DOI: 10.1175/JCLI-D-19-0026.1 (2019).

24. Weijer, W., Cheng, W., Garuba, O. A., Hu, A. & Nadiga, B. T. CMIP6 Models Predict Significant 21st Century Decline of the Atlantic Meridional Overturning Circulation. *Geophys. Res. Lett.* **47**, DOI: 10.1029/2019GL086075 (2020).

25. Caesar, L., Rahmstorf, S., Robinson, A., Feulner, G. & Saba, V. Observed fingerprint of a weakening atlantic ocean overturning circulation. *Nature* **556**, 191–196, DOI: 10.1038/s41586-018-0006-5 (2018).

26. Caesar, L., McCarthy, G., Thornalley, J., Cahill, N. & Rahmstorf, S. Current atlantic meridional overturning circulation weakest in last millennium. *Nat. Geosci.* **14**, 118–120, DOI: 10.1038/s41561-021-00699-z (2021).

27. Booth, B. B., Dunstone, N. J., Halloran, P. R., Andrews, T. & Bellouin, N. Aerosols implicated as a prime driver of twentieth-century north atlantic climate variability. *Nature* **484**, 228–232 (2012).

28. Buckley, M. W. & Marshall, J. Observations, inferences, and mechanisms of the Atlantic Meridional Overturning Circulation: A review. *Rev. Geophys.* **54**, 2015RG000493+, DOI: 10.1002/2015rg000493 (2016).

29. Yeager, S. G. & Robson, J. I. Recent progress in understanding and predicting atlantic decadal climate variability. *Curr. Clim. Chang. Reports* **3**, 112–127, DOI: 10.1007/s40641-017-0064-z (2017).

30. Moat, B. I. *et al.* Pending recovery in the strength of the meridional overturning circulation at 26°n. *Ocean. Sci.* **16**, 863–874, DOI: 10.5194/os-16-863-2020 (2020).

31. Kostov, Y. *et al.* Distinct sources of interannual subtropical and subpolar atlantic overturning variability. *Nat. Geosci.* DOI: 10.1038/s41561-021-00759-4 (2021).

32. Biastoch, A., Böning, C. W., Getzlaff, J., Molines, J.-M. & Madec, G. Causes of interannual–decadal variability in the Meridional Overturning Circulation of the midlatitude North Atlantic Ocean. *J. Clim.* **21**, 6599–6615, DOI: 10.1175/2008JCLI2404.1 (2008).

33. Yeager, S. & Danabasoglu, G. The Origins of Late-Twentieth-Century Variations in the Large-Scale North Atlantic Circulation. *J. Clim.* **27**, 3222–3247, DOI: 10.1175/jcli-d-13-00125.1 (2014).

34. Pillar, H. R., Heimbach, P., Johnson, H. L. & Marshall, D. P. Dynamical attribution of recent variability in Atlantic Overturning. *J. Clim.* **29**, 3339–3352, DOI: 10.1175/JCLI-D-15-0727.1 (2016).

35. Larson, S. M., Buckley, M. W. & Clement, A. C. Extracting the buoyancy-driven Atlantic meridional overturning circulation. *J. Clim.* DOI: 10.1175/JCLI-D-19-0590.1 (2020).

36. Baehr, J., Hirschi, J., Beismann, J.-O. & Marotzke, J. Monitoring the meridional overturning circulation in the north atlantic: A model-based array design study. *J. Mar. Res.* **62**, 283–312, DOI: doi:10.1357/0022240041446191 (2004).

37. Clément, L., Frajka-Williams, E., Szuts, Z. B. & Cunningham, S. A. Vertical structure of eddies and Rossby waves, and their effect on the Atlantic meridional overturning circulation at 26.5°N. *J. Geophys. Res. Ocean.* **119**, 6479–6498, DOI: 10.1002/2014JC010146 (2014).

38. Polo, I., Robson, J., Sutton, R. & Bamaseda, M. The importance of wind and buoyancy forcing of the boundary density variations and the geostrophic component of the AMOC at 26°N. *J. Phys. Oceanogr.* **44**, 2387–2408, DOI: 10.1175/JPO-D-13-0264.1 (2014).

39. Buckley, M. W., Ferreira, D., Campin, J.-M., Marshall, J. & Tulloch, R. On the relationship between decadal buoyancy anomalies and variability of the Atlantic Meridional Overturning Circulation. *J. Clim.* **25**, 8009–8030, DOI: 10.1175/JCLI-D-11-00505.1 (2012).

40. Bingham, R., Hughes, C., Roussenov, V. & Williams, R. Meridional coherence of the North Atlantic meridional overturning circulation. *Geophys. Res. Lett.* **34**, L23606, DOI: 10.1029/2007GL031731 (2007).

41. Mielke, C., Frajka-Williams, E. & Baehr, J. Observed and simulated variability of the AMOC at 26°N and 41°N. *Geophys. Res. Lett.* DOI: 10.1002/grl.50233 (2013).

42. Wunsch, C. & Heimbach, P. Two decades of the Atlantic Meridional Overturning Circulation: Anatomy, variations, extremes, prediction, and overcoming its limitations. *J. Clim.* **26**, 7167–7186, DOI: 10.1175/JCLI-D-12-00478.1 (2013).

43. Gu, S., Liu, Z. & Wu, L. Time scale dependence of the meridional coherence of the Atlantic Meridional Overturning Circulation. *J. Geophys. Res. Ocean.* **125**, e2019JC015838, DOI: 10.1029/2019JC015838 (2020).

44. Lozier, M., Roussenov, V., Reed, M. & Williams, R. Opposing decadal changes for the north atlantic meridional overturning circulation. *Nat. Geosci* **3**, 728—734, DOI: 10.1038/ngeo947 (2010).

45. Groeskamp, S. *et al.* The water mass transformation framework for ocean physics and biogeochemistry. *Annu. Rev. Mar. Sci.* **11**, 271–305, DOI: 10.1146/annurev-marine-010318-095421 (2019). PMID: 30230995.

46. Xu, X., Rhines, P. & Chassignet, E. On mapping the diapycnal water mass transformation of the upper north atlantic ocean. *J. Phys. Ocean.* **48**, 2233–2258, DOI: 10.1175/JPO-D-17-0223.1 (2018).

47. Böning, C. W., Scheinert, M., Dengg, J., Biastoch, A. & Funk, A. Decadal variability of subpolar gyre transport and its reverberation in the North Atlantic overturning. *Geophys. Res. Lett.* **33**, DOI: 10.1029/2006GL026906 (2006).

48. Robson, J., Sutton, R., Lohmann, K., Smith, D. & Palmer, M. D. Causes of the Rapid Warming of the North Atlantic Ocean in the Mid-1990s. *J. Clim.* **25**, 4116–4134, DOI: 10.1175/jcli-d-11-00443.1 (2012).

49. Delworth, T. L. & Zeng, F. The impact of the North Atlantic Oscillation on climate through its influence on the Atlantic Meridional Overturning Circulation. *J. Clim.* **29**, 941–962, DOI: 10.1175/JCLI-D-15-0396.1 (2016).

50. Kim, W. M., Yeager, S. & Danabasoglu, G. Atlantic Multidecadal Variability and associated climate impacts initiated by ocean thermohaline dynamics. *J. Clim.* **33**, 1317–1334, DOI: 10.1175/JCLI-D-19-0530.1 (2019).

51. Delworth, T., Manabe, S. & Stouffer, R. J. Interdecadal variations of the thermohaline circulation in a coupled ocean-atmosphere model. *J. Clim.* **6**, 1993–2011, DOI: 10.1175/1520-0442(1993)006<1993:IVOTTC>2.0.CO;2 (1993).

52. Kwon, Y.-O. & Frankignoul, C. Stochastically-driven multidecadal variability of the Atlantic meridional overturning circulation in CCSM3. *Clim. Dyn.* **38**, 859–876, DOI: 10.1007/s00382-011-1040-2 (2012).

53. Danabasoglu, G. *et al.* Variability of the Atlantic Meridional Overturning Circulation in CCSM4. *J. Clim.* **25**, 5153–5172, DOI: 10.1175/JCLI-D-11-00463.1 (2012).

54. Roberts, C. D., Garry, F. K. & Jackson, L. C. A multimodel study of sea surface temperature and subsurface density fingerprints of the Atlantic Meridional Overturning Circulation. *J. Clim.* **26**, 9155–9174, DOI: 10.1175/JCLI-D-12-00762.1 (2013).

55. Vage, K. *et al.* Surprising return of deep convection to the subpolar North Atlantic Ocean in winter 2007-2008. *Nat. Geosci* **2**, 67–72 (2009).

56. Rhein, M. *et al.* Deep water formation, the subpolar gyre, and the meridional overturning circulation in the subpolar North Atlantic. *Deep. Sea Res. Part II: Top. Stud. Oceanogr.* **58**, 1819–1832, DOI: 10.1016/j.dsr2.2010.10.061 (2011).

57. Yashayaev, I. & Loder, J. W. Recurrent replenishment of Labrador Sea Water and associated decadal-scale variability. *J. Geophys. Res. Ocean.* **121**, 8095–8114, DOI: 10.1002/2016jc012046 (2016).

58. Yashayaev, I. & Loder, J. W. Further intensification of deep convection in the Labrador Sea in 2016. *Geophys. Res. Lett.* **44**, 2016GL071668+, DOI: 10.1002/2016gl071668 (2017).

59. Li, F. *et al.* Subpolar north atlantic western boundary density anomalies and the meridional overturning circulation. *Nat Commun* **12**, 3002, DOI: 10.1038/s41467-021-23350-2 (2021).

60. Mauritzen, C. & Häkkinen, S. On the relationship between dense water formation and the "Meridional Overturning Cell" in the North Atlantic ocean. *Deep. Sea Res. Part I: Oceanogr. Res. Pap.* **46**, 877–894, DOI: 10.1016/S0967-0637(98)00094-6 (1999).

61. Deshayes, J., Frankignoul, C. & Drange, H. Formation and export of deep water in the Labrador and Irminger Seas in a GCM. *Deep. Sea Res. Part I: Oceanogr. Res. Pap.* **54**, 510 – 532, DOI: 10.1016/j.dsr.2006.12.014 (2007).

62. Grist, J. P., Marsh, R. & Josey, S. A. On the relationship between the north atlantic meridional overturning circulation and the surface-forced overturning streamfunction. *J. Clim.* **22**, 4989 – 5002, DOI: 10.1175/2009JCLI2574.1 (2009).

63. Josey, S. A., Grist, J. P. & Marsh, R. Estimates of meridional overturning circulation variability in the north atlantic from surface density flux fields. *J. Geophys. Res. Ocean.* **114**, DOI: https://doi.org/10.1029/2008JC005230 (2009).

64. Chafik, L. & Rossby, T. Volume, heat, and freshwater divergences in the Subpolar North Atlantic suggest the Nordic Seas as key to the state of the Meridional Overturning Circulation. *Geophys. Res. Lett.* **46**, 4799–4808, DOI: 10.1029/2019GL082110 (2019).

65. Lozier, M. S. *et al.* A sea change in our view of overturning in the subpolar North Atlantic. *Science* **363**, 516, DOI: 10.1126/science.aau6592 (2019).

66. Petit, T., Lozier, M. S., Josey, S. A. & Cunningham, S. A. Atlantic deep water formation occurs primarily in the Iceland Basin and Irminger Sea by local buoyancy forcing. *Geophys. Res. Lett.* **47** (2020).

67. Feucher, C., Garcia-Quintana, Y., Yashayaev, I., Hu, X. & Myers, P. G. Labrador Sea Water Formation rate and its impact on the local meridional overturning circulation. *J. Geophys. Res. Ocean.* **124**, 5654–5670, DOI: 10.1029/2019JC015065 (2019).

68. Hirschi, J. J. *et al.* The Atlantic Meridional Overturning Circulation in High-Resolution Models. *J. Geophys. Res. Ocean.* **125**, DOI: 10.1029/2019JC015522 (2020).

69. Menary, M. B., Jackson, L. C. & Lozier, M. S. Reconciling the relationship between the AMOC and Labrador Sea in OSNAP observations and climate models. *Geophys. Res. Lett.* **47**, DOI: https://doi.org/10.1029/2020GL089793 (2020).

70. Oldenburg, D., Wills, R., Armour, K., Thompson, L. & Jackson, L. Mechanisms of low-frequency variability in north atlantic ocean heat transport and amoc. *J Clim* (2021).

71. Hirschi, J. J.-M. *et al.* Chaotic variability of the meridional overturning circulation on subannual to interannual timescales. *Ocean. Sci.* **9**, 805–823, DOI: 10.5194/os-9-805-2013 (2013).

72. Grégorio, S. *et al.* Intrinsic variability of the Atlantic Meridional Overturning Circulation at interannual-to-multidecadal time scales. *J. Phys. Oceanogr.* **45**, 1929–1946, DOI: 10.1175/JPO-D-14-0163.1 (2015).

73. Leroux, S. *et al.* Intrinsic and atmospherically forced variability of the AMOC: Insights from a large-ensemble ocean hindcast. *J. Clim.* **31**, 1183–1203, DOI: 10.1175/JCLI-D-17-0168.1 (2018).

74. Frankcombe, L. M., von der Heydt, A. & Dijkstra, H. A. North Atlantic multidecadal climate variability: An investigation of dominant time scales and processes. *J. Clim.* **23**, 3626–3638, DOI: 10.1175/2010JCLI3471.1 (2010).

75. Sévellec, F. & Fedorov, A. V. The leading, interdecadal eigenmode of the Atlantic Meridional Overturning Circulation in a realistic ocean model. *J. Clim.* **26**, 2160–2183, DOI: 10.1175/JCLI-D-11-00023.1 (2012).

76. Huck, T., Arzel, O. & Sévellec, F. Multidecadal variability of the overturning circulation in presence of eddy turbulence. *J. Phys. Ocean.* **45**, 157–173, DOI: 10.1175/JPO-D-14-0114.1 (2014).

77. Rahmstorf, S. & Willebrand, J. The role of temperature feedback in stabilizing the thermohaline circulation. *J. Phys. Oceanogr.* **25**, 787–805, DOI: 10.1175/1520-0485(1995)025<0787:TROTFI>2.0.CO;2 (1995).

78. Jungclaus, J., Haak, H., Latif, M. & Mikolajewicz, U. Arctic–north atlantic interactions and multidecadal variability of the meridional overturning circulation. *J. Clim.* **18**, 4013 – 4031, DOI: 10.1175/JCLI3462.1 (2005).

79. Deshayes, J., Curry, R. & Msadek, R. Cmip5 model intercomparison of freshwater budget and circulation in the north atlantic. *J. Clim.* **27**, 3298 – 3317, DOI: 10.1175/JCLI-D-12-00700.1 (2014).

80. Timmermann, A., Latif, M., Voss, R. & Groetzner, A. Northern hemispheric interdecadal variability: a coupled air-sea mode. *J. Clim.* **11**, 1906–1931 (1998).

81. Dima, M. & Lohmann, G. A hemispheric mechanism for the Atlantic Multidecadal Oscillation. *J. Clim.* **20**, 2706–2719, DOI: 10.1175/JCLI4174.1 (2007).

82. Menary, M. B., Hodson, D. L. R., Robson, J. I., Sutton, R. T. & Wood, R. A. A mechanism of internal decadal Atlantic Ocean variability in a high-resolution coupled climate model. *J. Clim.* **28**, 7764–7785, DOI: 10.1175/JCLI-D-15-0106.1 (2015).

83. Menary, M. B. *et al.* Exploring the impact of cmip5 model biases on the simulation of north atlantic decadal variability. *Geophys. Res. Lett.* **42**, 5926–5934, DOI: https://doi.org/10.1002/2015GL064360 (2015). https://agupubs.onlinelibrary.wiley.com/doi/pdf/10.1002/2015GL064360.

84. Peings, Y., Simpkins, G. & Magnusdottir, G. Multidecadal fluctuations of the North Atlantic Ocean and feedback on the winter climate in CMIP5 control simulations. *J. Geophys. Res. Atmospheres* **121**, 2571–2592, DOI: 10.1002/2015JD024107 (2016). 2015JD024107.

85. Martin, T., Reintges, A. & Latif, M. Coupled north atlantic subdecadal variability in cmip5 models. *J. Geophys. Res. Ocean.* **124**, 2404–2417, DOI: https://doi.org/10.1029/2018JC014539 (2019). https://agupubs.onlinelibrary.wiley.com/doi/pdf/10.1029/2018JC014539.

86. Zhang, R. Latitudinal dependence of Atlantic meridional overturning circulation (AMOC) variations. *Geophys. Res. Lett.* **37**, L16703, DOI: 10.1029/2010GL044474 (2010).

87. Ortega, P. *et al.* Labrador sea sub-surface density as a precursor of multi-decadal variability in the north atlantic: a multi-model study. *Earth Syst. Dynam. Discuss. [preprint]* DOI: 10.5194/esd-2020-83 (2020).

88. Hodson, D. & Sutton, R. The impact of resolution on the adjustment and decadal variability of the Atlantic meridional overturning circulation in a coupled climate model. *Clim. Dyn.* **39**, 3057–3073, DOI: 10.1007/s00382-012-1309-0 (2012).

89. Getzlaff, J., Böning, C., Eden, C. & Biastoch, A. Signal propagation related to the North Atlantic overturning. *Geophys. Res. Lett.* **32**, DOI: 10.1029/2004GL021002 (2005).

90. Bower, A. S., Lozier, M. S., Gary, S. F. & Böning, C. W. Interior pathways of the North Atlantic meridional overturning circulation. *Nature* **459**, 243–247, DOI: 10.1038/nature07979 (2009).

91. Gary, S. F., Lozier, M. S., Biastoch, A. & Böning, C. W. Reconciling tracer and float observations of the export pathways of Labrador Sea Water. *Geophys. Res. Lett.* **39**, DOI: 10.1029/2012GL053978 (2012).

92. Rhein, M., Kieke, D. & Steinfeldt, R. Advection of North Atlantic Deep Water from the Labrador Sea to the southern hemisphere. *J. Geophys. Res. Ocean.* **120**, 2471–2487, DOI: 10.1002/2014JC010605 (2015).

93. Zou, S. & Lozier, M. S. Breaking the linkage between Labrador Sea Water production and its advective export to the subtropical gyre. *J. Phys. Oceanogr.* **46**, 2169–2182, DOI: 10.1175/JPO-D-15-0210.1 (2016).

94. Li, F. *et al.* Local and downstream relationships between Labrador Sea Water volume and North Atlantic Meridional Overturning Circulation variability. *J. Clim.* **32**, 3883–3898, DOI: 10.1175/JCLI-D-18-0735.1 (2019).

95. Bryden, H. L., Longworth, H. R. & Cunningham, S. A. Slowing of the Atlantic meridional overturning circulation at 25°N. *Nature* **438**, 655–657, DOI: 10.1038/nature04385 (2005).

96. Mercier, H. *et al.* Variability of the meridional overturning circulation at the greenland–portugal ovide section from 1993 to 2010. *Prog. Oceanogr.* **132**, 250 – 261, DOI: https://doi.org/10.1016/j.pocean.2013.11.001 (2015).

97. Kanzow, T. *et al.* Seasonal variability of the Atlantic meridional overturning circulation at 26.5°N. *J. Clim.* **23**, 5678–5698, DOI: 10.1175/2010JCLI3389.1 (2010).

98. Frajka-Williams, E. *et al.* Atlantic meridional overturning circulation observed by the rapid-mocha-wbts (rapid-meridional overturning circulation and heatflux array-western boundary time series) array at 26n from 2004 to 2020 (v2020.1), DOI: 10.5285/cc1e34b3-3385-662b-e053-6c86abc03444 (2021).

99. Rayner, N. A. *et al.* Global analyses of sea surface temperature, sea ice, and night marine air temperature since the late nineteenth century. *J. Geophys. Res.* **108**, 4407, DOI: 10.1029/2002JD002670. (2003).

100. Willis, J. K. Can in situ floats and satellite altimeters detect long-term changes in atlantic ocean overturning? geophys. res. lett., 37, l06602, doi:10.1029/2010gl042372. *Geophys. Res. Lett.* **37**, L06602, DOI: 10.1029/2010GL042372 (2010).

101. Frajka-Williams, E. Estimating the Atlantic overturning at 26°N using satellite altimetry and cable measurements. *Geophys. Res. Lett.* **42**, 2015GL063220+, DOI: 10.1002/2015gl063220 (2015).

102. Sanchez-Franks, A., Frajka-Williams, E., Moat, B. I. & Smeed, D. A. A dynamically based method for estimating the atlantic meridional overturning circulation at 26n from satellite altimetry. *Ocean. Sci.* **17**, 1321–1340, DOI: 10.5194/os-17-1321-2021 (2021).

103. WALIN, G. On the relation between sea-surface heat flow and thermal circulation in the ocean. *Tellus* **34**, 187–195, DOI: https://doi.org/10.1111/j.2153-3490.1982.tb01806.x (1982).

104. Marsh, R., Josey, S. A., de Nurser, A. J. G., Cuevas, B. A. & Coward, A. C. Water mass transformation in the north atlantic over 1985-2002 simulated in an eddy-permitting model. *Ocean. Sci.* **1**, 127–144, DOI: 10.5194/os-1-127-2005 (2005).

105. Large, W. G. & Yeager, S. The global climatology of an interannually varying air-sea flux data set. *Clim. Dyn.* **33**, 341–364 (2009).

106. Tsujino, H. *et al.* JRA-55 based surface dataset for driving ocean–sea-ice models (JRA55-do). *Ocean. Model.* **130**, 79–139, DOI: 10.1016/j.ocemod.2018.07.002 (2018).

107. Storto, A. *et al.* Ocean reanalyses: Recent advances and unsolved challenges. *Front. Mar. Sci.* **6**, 418, DOI: 10.3389/fmars.2019.00418 (2019).

108. Fox-Kemper, B. *et al.* Challenges and prospects in ocean circulation models. *Front. Mar. Sci.* **6**, DOI: 10.3389/fmars.2019.00065 (2019).

109. Chassignet, E. P. *et al.* Impact of horizontal resolution on global ocean–sea ice model simulations based on the experimental protocols of the ocean model intercomparison project phase 2 (omip-2). *Geosci. Model. Dev.* **13**, 4595–4637, DOI: 10.5194/gmd-13-4595-2020 (2020).

110. Biastoch, A. *et al.* Regional imprints of changes in the atlantic meridional overturning circulation in the eddy-rich ocean model viking20x. *Ocean. Sci.* **17**, 1177–1211, DOI: 10.5194/os-17-1177-2021 (2021).

111. Danabasoglu, G. *et al.* North Atlantic simulations in Coordinated Ocean-ice Reference Experiments phase II (CORE-II). Part I: Mean states. *Ocean. Model.* **73**, 76–107, DOI: 10.1016/j.ocemod.2013.10.005 (2014).

112. Danabasoglu, G. *et al.* North Atlantic simulations in Coordinated Ocean-ice Reference Experiments phase II (CORE-II). Part II: Inter-annual to decadal variability. *Ocean. Model.* **97**, 65–90, DOI: 10.1016/j.ocemod.2015.11.007 (2016).

113. Blaker, A. *et al.* Historical analogues of the recent extreme minima observed in the Atlantic meridional overturning circulation at 26°N. *Clim. Dyn.* **44**, 457–473, DOI: 10.1007/s00382-014-2274-6 (2015).

114. Griffies, S. M. *et al.* Coordinated Ocean-ice Reference Experiments (CORES). *Ocean. Model.* **26**, 1–46, DOI: 10.1016/j.ocemod.2008.08.007 (2009).

115. Behrens, E., Biastoch, A. & Böning, C. W. Spurious AMOC trends in global ocean sea-ice models related to subarctic freshwater forcing. *Ocean. Model.* **69**, 39–49, DOI: 10.1016/j.ocemod.2013.05.004 (2013).

116. Riser, S. C. *et al.* Fifteen years of ocean observations with the global Argo array. *Nat. Clim. Chang.* **6**, 145–153, DOI: 10.1038/nclimate2872 (2016).

117. Karspeck, A. R. *et al.* Comparison of the Atlantic meridional overturning circulation between 1960 and 2007 in six ocean reanalysis products. *Clim. Dyn.* 1–26, DOI: 10.1007/s00382-015-2787-7 (2015).

118. Roberts, C. D. & Palmer, M. D. Detectability of changes to the Atlantic Meridional Overturning Circulation in the Hadley Centre Climate Models. *Clim. Dyn.* **39**, 2533–2546, DOI: 10.1007/s00382-012-1306-3 (2012).

119. Jackson, L. & Wood, R. Fingerprints for early detection of changes in the amoc. *J. Clim.* **33**, 7027–7044, DOI: 10.1175/JCLI-D-20-0034.1 (2020).

120. Latif, M. *et al.* Reconstructing, monitoring, and predicting multidecadal-scale changes in the north atlantic thermohaline circulation with sea surface temperature. *J. Clim.* **17**, 1605–1614, DOI: 10.1175/1520-0442(2004)017<1605:RMAPMC>2.0.CO;2 (2004).

121. Msadek, R., Dixon, K. W., Delworth, T. L. & Hurlin, W. Assessing the predictability of the atlantic meridional overturning circulation and associated fingerprints. *Geophys. Res. Lett* **37**, L19608, DOI: 10.1029/2010GL044517 (2010).

122. Zhang, L. & Wang, C. Multidecadal North Atlantic sea surface temperature and Atlantic meridional overturning circulation variability in CMIP5 historical simulations. *J. Geophys. Res. Ocean.* **118**, 5772–5791, DOI: 10.1002/jgrc.20390 (2013).

123. Rahmstorf, S. *et al.* Exceptional twentieth-century slowdown in Atlantic Ocean overturning circulation. *Nat. Clim. Chang.* **5**, 475–480, DOI: 10.1038/nclimate2554 (2015).

124. Robson, J., Hodson, D., Hawkins, E. & Sutton, R. Atlantic overturning in decline? *Nat. Geosci.* **7**, 2–3, DOI: 10.1038/ngeo2050 (2013).

125. MacCarthy, G. D., Haigh, I. D., Hirschi, J. J.-M., Grist, J. P. & Smeed, D. A. Ocean impact on decadal atlantic climate variability revealed by sea-level observations. *Nature* **521**, 508–510 (2015).

126. Diabaté, S. T. *et al.* Western boundary circulation and coastal sea-level variability in northern hemisphere oceans. *Ocean. Sci.* **17**, 1449–1471, DOI: 10.5194/os-17-1449-2021 (2021).

127. Thornalley, D. J. R. *et al.* Anomalously weak labrador sea convection and atlantic overturning during the past 150 years. *Nature* **556**, 227–230, DOI: 10.1038/s41586-018-0007-4 (2018).

128. Zantopp, R., Fischer, J., Visbeck, M. & Karstensen, J. From interannual to decadal: 17 years of boundary current transports at the exit of the Labrador Sea. *J. Geophys. Res. Ocean.* **122**, 1724–1748, DOI: 10.1002/2016JC012271 (2017).

129. Handmann, P. *et al.* The Deep Western Boundary Current in the Labrador Sea From Observations and a High-Resolution Model. *J. Geophys. Res. Ocean.* **123**, 2829–2850, DOI: 10.1002/2017JC013702 (2018).

130. Osterhus, S. *et al.* Arctic Mediterranean exchanges: a consistent volume budget and trends in transports from two decades of observations. *Ocean. Sci.* **15**, 379–399, DOI: 10.5194/os-15-379-2019 (2019).

131. Delworth, T. L. & Dixon, K. W. Have anthropogenic aerosols delayed a greenhouse gas-induced weakening of the north atlantic thermohaline circulation? *Geophys. Res. Lett.* **33**, L02606, DOI: 10.1029/2005GL024980 (2006).

132. Robson, J., T, S. R., Archibald, A. & et al. Recent multivariate changes in the north atlantic climate system, with a focus on 2005- 2016. *Int J Clim.* DOI: 10.1002/joc.5815 (2018).

133. Holliday, N. *et al.* Ocean circulation causes the largest freshening event for 120 years in eastern subpolar north atlantic. *Nat. Comms* **11**, 585 (2020).

134. Rühs, S. *et al.* Changing spatial patterns of deep convection in the subpolar North Atlantic. *J. Geophys. Res. Ocean.* **126**, e2021JC017245, DOI: 10.1029/2021jc017245 (2021).

135. Häkkinen, S. A simulation of thermohaline effects of a great salinity anomaly. *J. Clim.* **12**, 1781 – 1795, DOI: 10.1175/1520-0442(1999)012<1781:ASOTEO>2.0.CO;2 (1999).

136. Haak, H., Jungclaus, J., Mikolajewicz, U. & Latif, M. Formation and propagation of great salinity anomalies. *Geophys. Res. Lett.* **30**, 1473, DOI: https://doi.org/10.1029/2003GL017065 (2003).

137. Kim, W. M., Yeager, S. & Danabasoglu, G. Revisiting the causal connection between the great salinity anomaly of the 1970s and the shutdown of labrador sea deep convection. *J. Clim.* **34**, 675—696, DOI: 10.1175/JCLI-D-20-0327.1 (2021).

138. Chen, X. & Tung, K. Global surface warming enhanced by weak atlantic overturning circulation. *Nature* **559**, 387—391, DOI: /10.1038/s41586-018-0320-y (2018).

139. Roberts, C. D., Jackson, L. & McNeall, D. Is the 2004-2012 reduction of the Atlantic meridional overturning circulation significant? *Geophys. Res. Lett.* **41**, 3204–3210, DOI: 10.1002/2014gl059473 (2014).

140. McCarthy, G. *et al.* Observed interannual variability of the Atlantic MOC at 26.5°N. *Geophys. Res. Lett.* **39**, L19609, DOI: 10.1029/2012GL052933 (2012).

141. Roberts, C. D. *et al.* Atmosphere drives recent interannual variability of the Atlantic meridional overturning circulation at 26.5°N. *Geophys. Res. Lett.* **40**, 5164–5170, DOI: 10.1002/grl.50930 (2013).

142. Zhao, J. & Johns, W. Wind-forced interannual variability of the atlantic meridional overturning circulation at 26.5°n. *J. Geophys. Res. Ocean.* **119**, 2403–2419, DOI: https://doi.org/10.1002/2013JC009407 (2014).

143. Frajka-Williams, E., Lankhorst, M., Koelling, J. & Send, U. Coherent Circulation Changes in the Deep North Atlantic From 16N and 26N Transport Arrays. *J. Geophys. Res. - Ocean.* https://doi.org/10.1029/2018JC013949+ (2018).

144. Piecuch, C. G., Ponte, R. M., Little, C. M., Buckley, M. W. & Fukumori, I. Mechanisms underlying recent decadal changes in subpolar north atlantic ocean heat content. *J. Geophys. Res. Ocean.* **122**, 7181–7197, DOI: 10.1002/2017JC012845 (2017).

145. Tesdal, J.-E. & Haine, T. W. N. Dominant terms in the freshwater and heat budgets of the subpolar north atlantic ocean and nordic seas from 1992 to 2015. *J. Geophys. Res. Ocean.* **125**, e2020JC016435, DOI: https://doi.org/10.1029/2020JC016435 (2020).

146. Zhang, R. Coherent surface-subsurface fingerprint of the Atlantic meridional overturning circulation. *Geophys. Res. Lett.* **35**, L20705+, DOI: 10.1029/2008gl035463 (2008).

147. Zhang, J. & Zhang, R. On the evolution of atlantic meridional overturning circulation fingerprint and implications for decadal predictability in the north atlantic. *Geophys. Res. Lett.* **42**, 5419–5426, DOI: 10.1002/2015GL064596 (2015).

148. Josey, S. A. *et al.* The recent atlantic cold anomaly: Causes, consequences, and related phenomena. *Annu. Rev. Mar. Sci.* **10**, 475–501, DOI: 10.1146/annurev-marine-121916-063102 (2018). PMID: 28934597.

149. Desbruyères, D., Chafik, L. & Maze, G. A shift in the ocean circulation has warmed the subpolar north atlantic ocean since 2016. *Nat. Commun Earth Environ* **2**, 48, DOI: 10.1038/s43247-021-00120-y (2021).

150. Moat, B. *et al.* Insights into decadal North Atlantic sea surface temperature and ocean heat content variability from an eddy-permitting coupled climate model. *J. Clim.* **32**, 6137–6149, DOI: 10.1175/JCLI-D-18-0709.1 (2019).

151. Clement, A. *et al.* The Atlantic Multidecadal Oscillation without a role for ocean circulation. *Science* **350**, 320–324 (2015).

152. Cane, M. A., Clement, A. C., Murphy, L. N. & Bellomo, K. Low-pass filtering, heat flux, and Atlantic multidecadal variability. *J. Clim.* **30**, 7529–7553, DOI: 10.1175/JCLI-D-16-0810.1 (2017).

153. Murphy, L. N., Bellomo, K., Cane, M. & Clement, A. The role of historical forcings in simulating the observed atlantic multidecadal oscillation. *Geophys. Res. Lett.* **44**, 2472–2480, DOI: https://doi.org/10.1002/2016GL071337 (2017).

154. Yan, X., Zhang, R. & Knutson, T. R. Underestimated AMOC Variability and Implications for AMV and Predictability in CMIP Models. *Geophys. Res. Lett.* **45**, 4319–4328 (2018).

155. Gregory, J. M. *et al.* A model intercomparison of changes in the Atlantic thermohaline circulation in response to increasing atmospheric CO-2 concentration. *Geophys. Res. Lett.* **32**, DOI: 10.1029/2005GL023209 (2005).

156. Marshall, J., Donohoe, A., Ferreira, D. & McGee, D. The ocean's role in setting the mean position of the Inter-Tropical Convergence Zone. *Clim. Dyn.* **42**, 1967–1979, DOI: 10.1007/s00382-013-1767-z (2014).

157. Sévellec, F., Fedorov, A. & Liu, W. Arctic sea-ice decline weakens the atlantic meridional overturning circulation. *Nat. Clim Chang.* **7**, 604—610, DOI: 10.1038/nclimate3353 (2017).

158. Hassan, T., Allen, R. J., Liu, W. & Randles, C. A. Anthropogenic aerosol forcing of the atlantic meridional overturning circulation and the associated mechanisms in cmip6 models. *Atmospheric Chem. Phys.* **21**, 5821–5846, DOI: 10.5194/acp-21-5821-2021 (2021).

159. Menary, M. B. *et al.* Mechanisms of aerosol-forced amoc variability in a state of the art climate model. *J. Geophys. Res. Ocean.* **118**, 2087–2096, DOI: 10.1002/jgrc.20178 (2013).

160. Smith, C. J. *et al.* Energy budget constraints on the time history of aerosol forcing and climate sensitivity. *J. Geophys. Res. Atmospheres* **126**, e2020JD033622, DOI: https://doi.org/10.1029/2020JD033622 (2021). E2020JD033622 2020JD033622, https://agupubs.onlinelibrary.wiley.com/doi/pdf/10.1029/2020JD033622.

161. Wang, C., Soden, B. J., Yang, W. & Vecchi, G. A. Compensation between cloud feedback and aerosol-cloud interaction in cmip6 models. *Geophys. Res. Lett.* **48**, e2020GL091024, DOI: https://doi.org/10.1029/2020GL091024 (2021). E2020GL091024 2020GL091024, https://agupubs.onlinelibrary.wiley.com/doi/pdf/10.1029/2020GL091024.

162. Zhu, C. & Liu, Z. Weakening atlantic overturning circulation causes south atlantic salinity pile-up. *Nat. Clim. Chang.* DOI: 10.1038/s41558-020-0897-7 (2020).

163. Piecuch, C. Likely weakening of the florida current during the past century revealed by sea-level observations. *Nat Commun* **11**, DOI: 10.1038/s41467-020-17761-w (2020).

164. Moffa-Sánchez, P. *et al.* Variability in the northern north atlantic and arctic oceans across the last two millennia: A review. *Paleoceanogr. Paleoclimatology* **34**, 1399–1436, DOI: 10.1029/2018PA003508 (2019).

165. Little, C. M., Zhao, M. & Buckley, M. W. Do surface temperature indices reflect centennial-timescale trends in atlantic meridional overturning circulation strength?. *Geophys. Res. Lett.* **47**, e2020GL090888, DOI: 10.1029/2020GL090888 (2020).

166. Boning, C. W., Behrens, E., Biastoch, A., Getzlaff, K. & Bamber, J. L. Emerging impact of Greenland meltwater on deepwater formation in the North Atlantic Ocean. *Nat. Geosci.* **9**, 523–527, DOI: 10.1038/ngeo2740 (2016).

167. van den Berk, J. & Drijfhout, S. A realistic freshwater forcing protocol for ocean-coupled climate models. *Ocean. Model.* **81**, 36–48, DOI: https://doi.org/10.1016/j.ocemod.2014.07.003 (2014).

168. Reintges, A., Martin, T., Latif, M. & Keenlyside, N. Uncertainty in twenty-first century projections of the Atlantic Meridional Overturning Circulation in CMIP3 and CMIP5 models. *Clim. Dyn.* 1–17, DOI: 10.1007/s00382-016-3180-x (2016).

169. Liu, W., Xie, S.-P., Liu, Z. & Zhu, J. Overlooked possibility of a collapsed atlantic meridional overturning circulation in warming climate. *Sci. Adv.* **3**, e1601666, DOI: 10.1126/sciadv.1601666 (2017). https://www.science.org/doi/pdf/10.1126/sciadv.1601666.

170. Jackson, L. C. *et al.* Impact of ocean resolution and mean state on the rate of amoc weakening. *Clim. Dyn.* **55**, 1711–1732, DOI: 10.1007/s00382-020-05345-9 (2020).

171. Chang, P. *et al.* An unprecedented set of high-resolution earth system simulations for understanding multiscale interactions in climate variability and change. *J. Adv. Model. Earth Syst.* **12**, e2020MS002298, DOI: https://doi.org/10.1029/2020MS002298 (2020).

172. Pohlmann, H. *et al.* Predictability of the mid-latitude Atlantic meridional overturning circulation in a multi-model system. *Clim. Dyn.* **41**, 775–785, DOI: 10.1007/s00382-013-1663-6 (2013).

173. Global annual to decadal climate update. Tech. Rep., World Meteorological Organisation, Geneva, Switzerland (2020).

174. Yeager, S. The abyssal origins of north atlantic decadal predictability. *Clim. Dyn.* **55**, 2253–2271, DOI: 10.1007/s00382-020-05382-4 (2020).

175. Worthington, E. L. *et al.* A 30-year reconstruction of the atlantic meridional overturning circulation shows no decline. *Ocean. Sci.* **17**, 285–299, DOI: 10.5194/os-17-285-2021 (2021).

176. Cunningham, S. A. *et al.* Atlantic Meridional Overturning Circulation slowdown cooled the subtropical ocean. *Geophys. Res. Lett.* **40**, 2013GL058464+, DOI: 10.1002/2013gl058464 (2013).

177. Zou, S., Lozier, M., Li, F., Abernathy, R. & Jackson, L. Density-compensated overturning in the labrador sea. *Nature. Geosci.* **13**, 121–126, DOI: 10.1038/s41561-019-0517-1 (2020).

178. Frajka-Williams, E. *et al.* Atlantic meridional overturning circulation: Observed transport and variability. *Front. Mar. Sci.* **6**, DOI: 10.3389/fmars.2019.00260 (2019).

179. Good, S. A., Martin, M. J. & Rayner, N. A. EN4: Quality controlled ocean temperature and salinity profiles and monthly objective analyses with uncertainty estimates. *J. Geophys. Res.* **118**, 6704–6716 (2013).

180. Spall, M. A. Boundary currents and watermass transformation in marginal seas. *J. Phys. Ocean.* **34**, 1197–1213, DOI: 10.1175/1520-0485(2004)034<1197:BCAWTI>2.0.CO;2 (2004).

181. Sayol, J.-M., Dijkstra, H. & Katsman, C. Seasonal and regional variations of sinking in the subpolar north atlantic from a high-resolution ocean model. *Ocean. Sci.* **15**, 1033–1053, DOI: 10.5194/os-15-1033-2019 (2019).

182. Marshall, J. & Speer, K. Closure of the meridional overturning circulation through Southern Ocean upwelling. *Nat. Geosci* **5**, 171–180, DOI: 10.1038/ngeo1391 (2012).

Acknowledgements

LCJ was supported by the Met Office Hadley Centre Climate Programme funded by BEIS and Defra (GA01101). MWB gratefully acknowledges the support from the NOAA ESS Program (NA20OAR4310396) and the NASA Physical Oceanography Program (80NSSC20K0823). JR was supported by NERC through NCAS, and through the NERC ACSIS project (NE/N018001/1), and the UKRI-NERC WISHBONE (NE/T013516/1) and SNAP-DRAGON (NE/T013494/1) projects. EFW and BM were supported by the UK Natural Environment Research Council RAPID-AMOC programme at 26.5^{o}N. BM was also supported by the European Union Horizon 2020 research and innovation programme BLUE-ACTION (Grant 727852). The authors thank Herlé Mercier, Alejandra Sanchez-Franks and Gerard McCarthy for providing updated time series for the AMOC at A25-Ovide, AMOC at 26.5^{o}N, and sea level proxy respectively.

Author contributions

LCJ led the writing, coordinated the contributions and made the figures. All authors discussed the content and contributed to the writing of the manuscript.

Competing interests

The authors declare no competing interests.

Peer review information

Nature Reviews Earth & Environment thanks the anonymous reviewers for their contribution to the peer review of this work.

Supplementary information

Supplementary information is available for this paper at https://doi.org/10.1038/s415XX-XXX-XXXX-X

Publishers note

Springer Nature remains neutral with regard to jurisdictional claims in published maps and institutional affiliations.

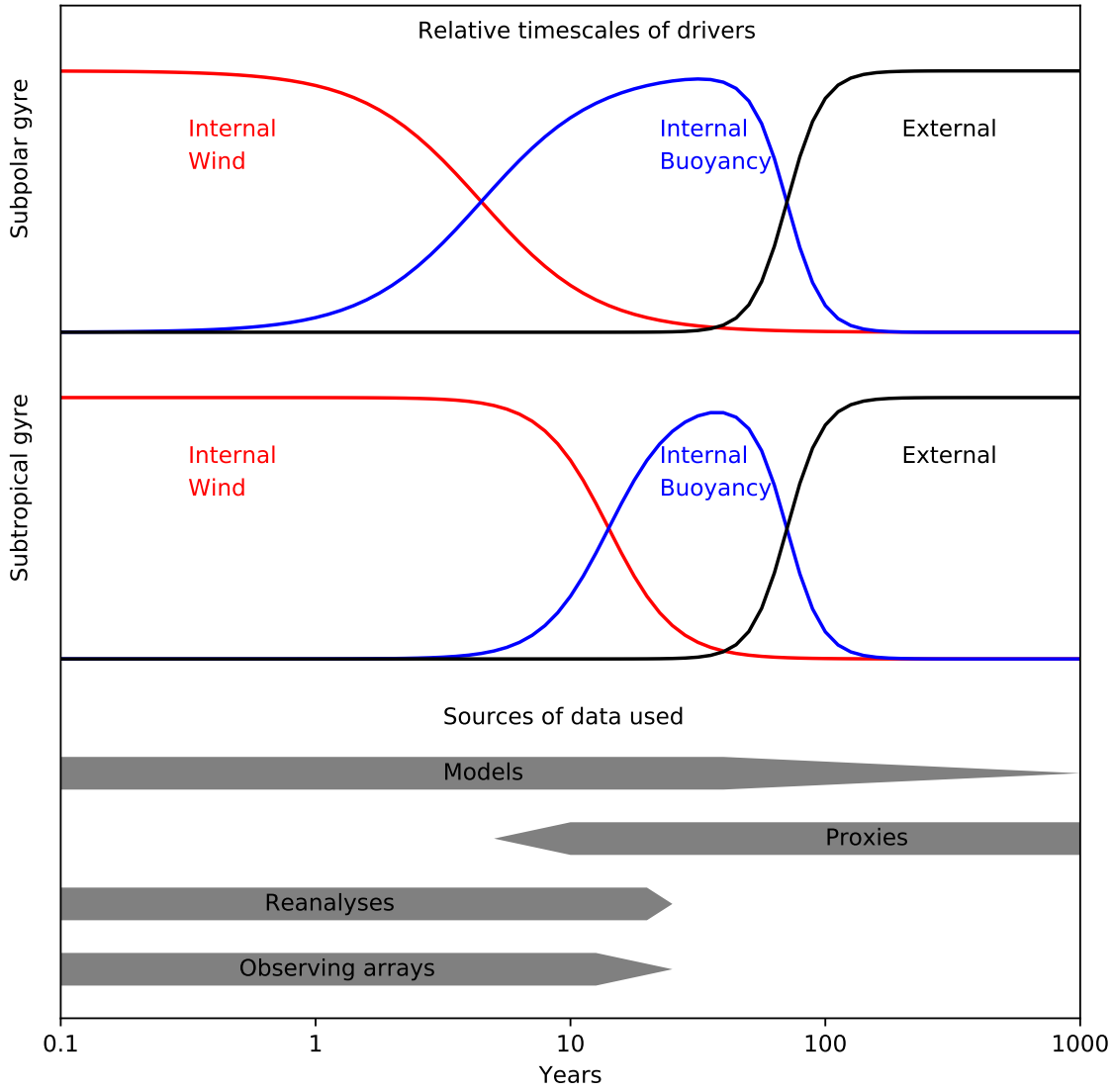

Figure 1. Schematic of AMOC timescales. a| Relative contributions of internal wind, buoyancy forcing and external forcing for AMOC changes in the subpolar North Atlantic. b| As in a, but for the subtropical North Atlantic. c| Timescale over which different data sources are able to distinguish AMOC variability based on their length (see Supplementary Information), and assuming that proxies used do not represent higher frequency AMOC variability. Drivers of AMOC variability differ depending on timescales, and different data sources are appropriate for different timescales.

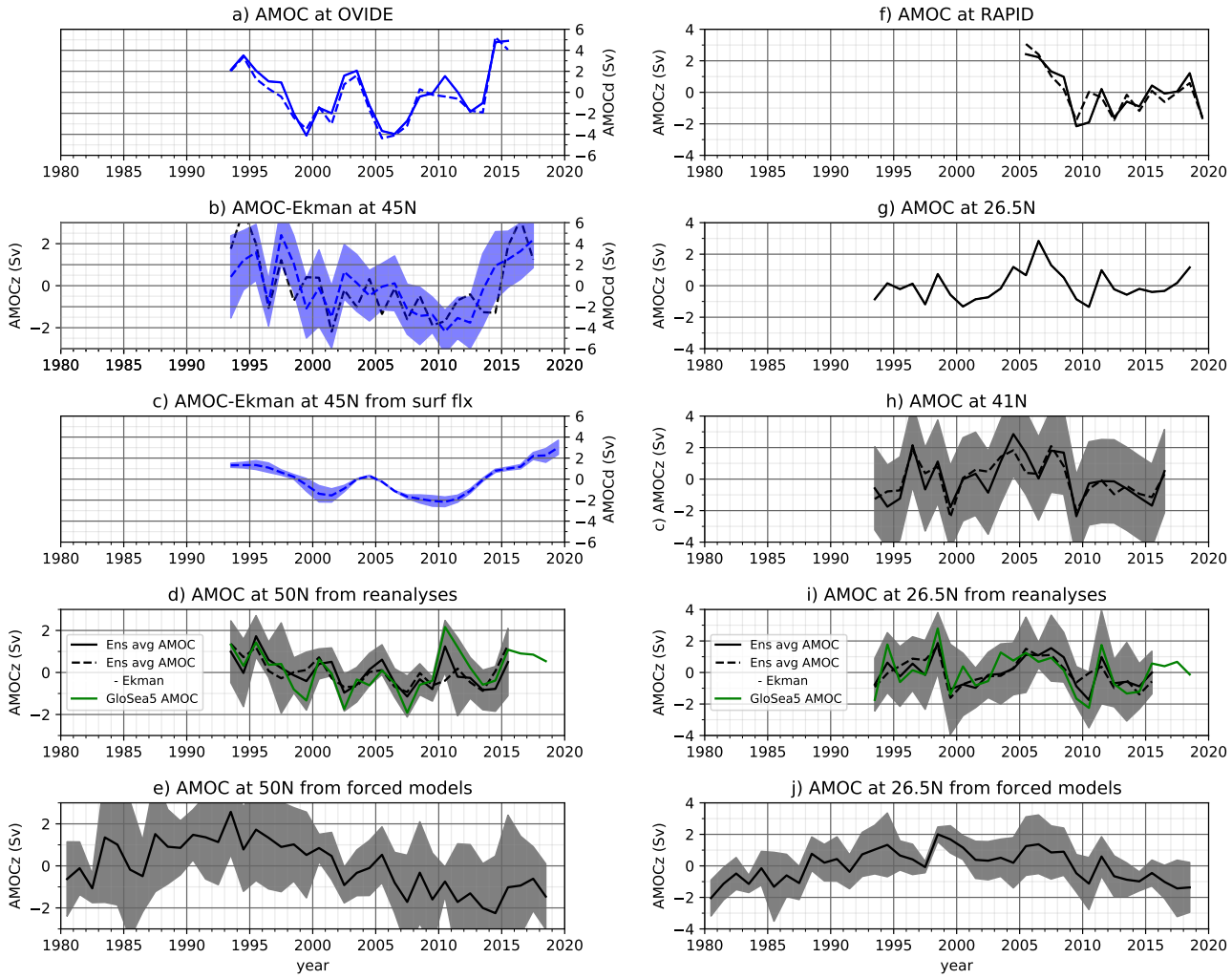

Figure 2. Timeseries of AMOC anomalies. Reconstructed AMOC in the subpolar North Atlantic (left): a| AMOC from observations along the Portugal-Greenland A25-OVIDE line[96]; b| AMOC from observations at 45^{o}N[12]; c| Implied overturning in density space from observed surface fluxes[12]; d| AMOC at 50^{o}N from an ensemble mean of ocean reanalyses[13] (black) and GloSea5 reanalysis[20] (green); e| AMOC at 50^{o}N from forced models participating in OMIP2 (ref[14]). Reconstructed AMOC in the subtropical North Atlantic (right): f| AMOC at 26.5^{o}N from the RAPID array[98]; g| AMOC from observations at 26.5^{o}N[102]; h| AMOC from observations at 41^{o}N[100]; i| as in d but for the AMOC at 26.5^{o}N; j| as e but for the AMOC at 26.5^{o}N. AMOC is either the maximum of the overturning in density space (blue, right axis) or the maximum in depth space (black, left axis). Dashed lines indicate those timeseries wherein the wind-driven Ekman component is excluded. Shading indicates observational uncertainties for b, c and h, or 2 times the standard deviation for d, e, i and j. See Supplementary Information for more detail on data sources. AMOC timeseries in the subpolar and subtropical North Atlantic show changes on interannual to decadal timescales.

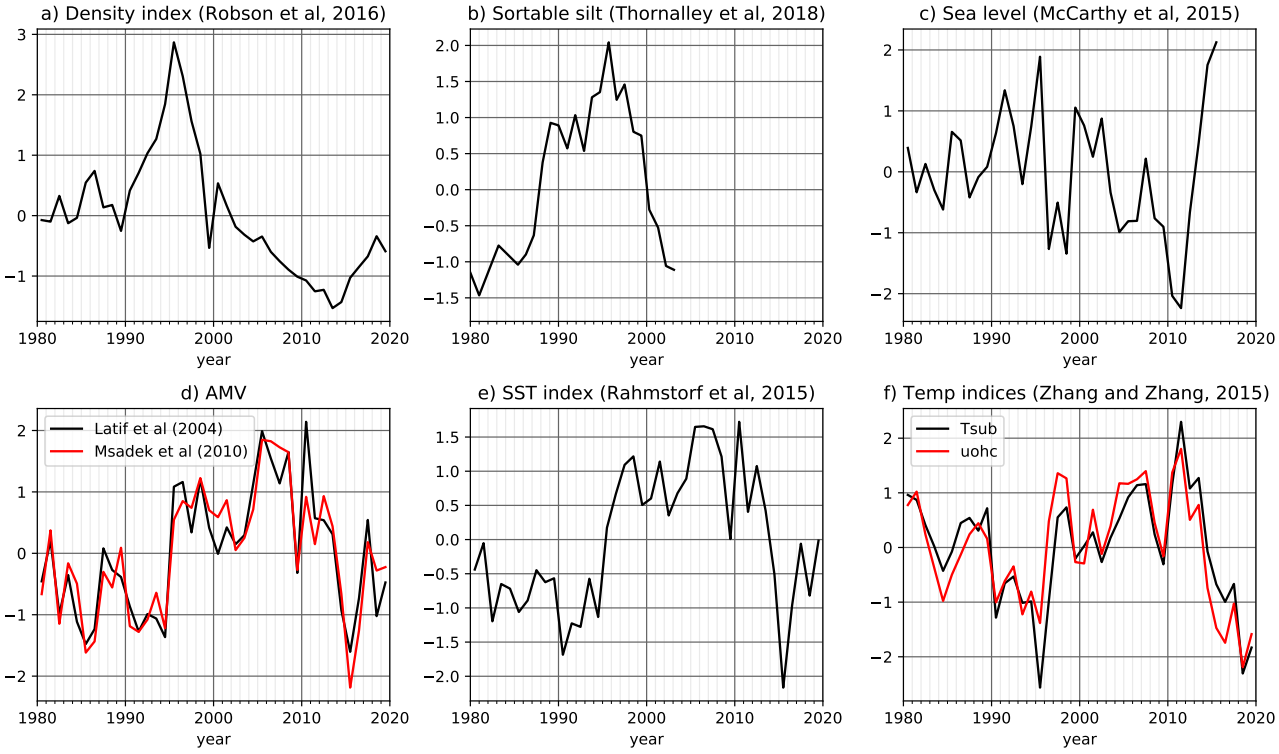

Figure 3. AMOC proxy records from 1980. a| Labrador Sea density proxy[15]; b| Sortable silt (proxy of deep boundary current speed)[127]; c| Sea level proxy[125,126]; d| Indices of Atlantic Multidecadal Variability from ref[120] (black) and ref[121] (red); e| Subpolar sea surface temperature (SST) proxy[123]; f| Temperature indices, including temperature at 400 m (T_{sub}; black) and ocean heat content over the top 700 m (uohc; red)[147]. All proxies are presented as standardised anomalies (see Supplementary Information). AMOC proxies support a strong subpolar AMOC in the mid 90s and weak in the early 2010s.

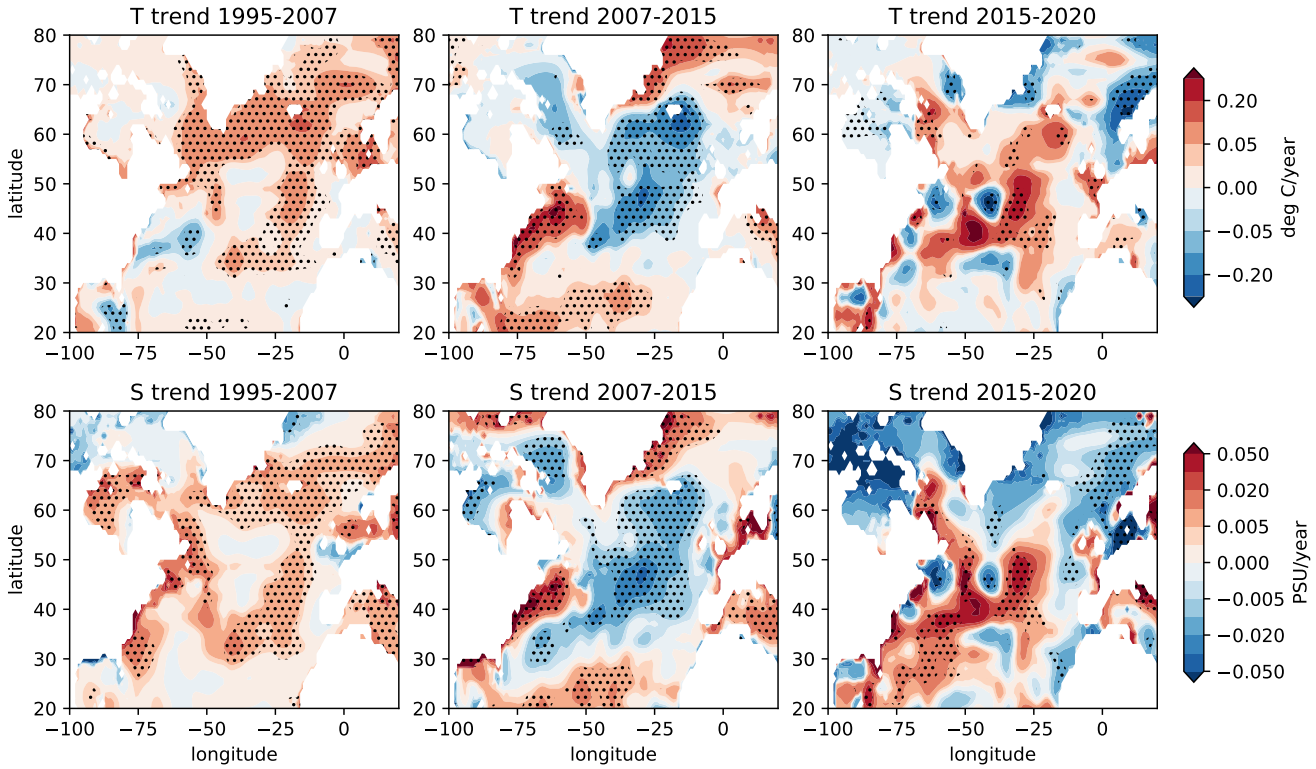

Figure 4. North Atlantic temperature and salinity trends. Trends of temperature averaged over the top 700 m for years 1995–2007 (panel a), 2007-2015 (panel b) and 2015–2020 (panel c). Trends of salinity averaged over the top 700 m for years 1995–2007 (panel d), 2007–2015 (panel e) and 2015–2020 (panel f). Stippling indicates statistically significant trends (P<0.05). Analysis and regions adapted from ref[15] and calculated from EN4 data[179]. Atlantic temperature and salinity trends reveal periods of warming and salinification (1995–2007, 2015–2020) and cooling and freshening (2007–2015).

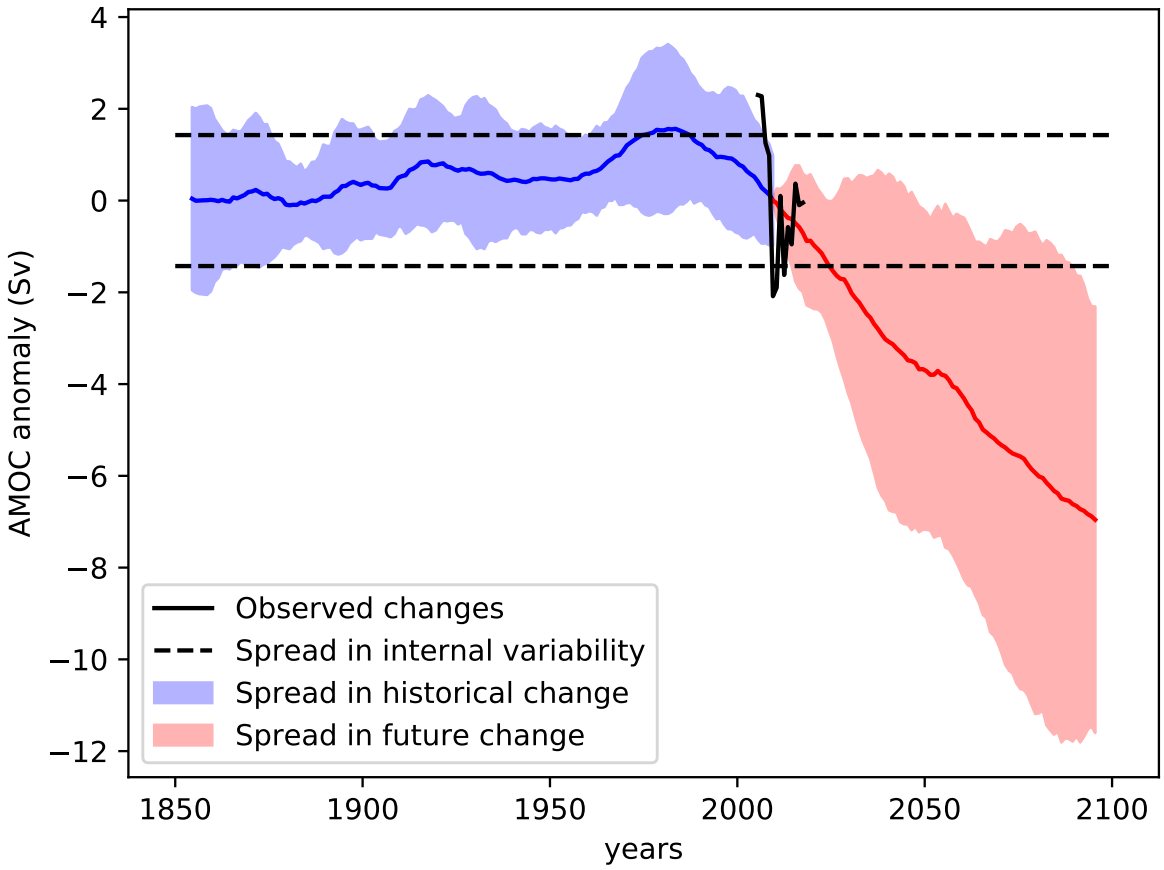

Figure 5. Past and future AMOC changes from climate models. Annual mean observed AMOC anomalies from RAPID[98] (black). The ensemble mean and spread (2*standard deviation) of 10 year running mean AMOC anomalies in the CMIP6 historical scenario (blue line and shading). The ensemble mean and spread (2*standard deviation) of 10 year running mean AMOC projections for the scenario SSP585 from CMIP6 (red line and shading). For modelled scenarios, the mean illustrates the forced response to changes in greenhouse gases and aerosols, and the spread includes differences in forced response and internal variability. See Supplementary Information for more detail on data sources. The black horizontal lines indicates internal variability of the AMOC, calculated as two times the ensemble mean standard deviation of 10 year mean AMOC in the CMIP6 preindustrial control experiment. The AMOC is projected to weaken in the future, however internal variability could obscure this signal.

BOX: Introduction to the AMOC

The Atlantic Meridional Overturning Circulation (AMOC) is a system of currents in the North Atlantic, whose net effect is to transport warmer upper waters (above 1000 m) northwards and colder deep waters (1000–3000 m) southwards (see dark and light grey arrows on Figure, respectively). The Gulf Stream and its extension into the North Atlantic current are major contributions to the upper limb of the AMOC, as are the recirculations in oceanic gyres and transports by mesoscale eddies (typical currents shown in upper and front faces of Figure). As light, upper waters are transported north from the tropics, they lose heat and hence become denser. Once the waters have reached the Irminger, Labrador or Greenland-Iceland-Norwegian Seas, stratification between upper and lower waters is reduced enough to trigger deep convection in winter, generating sinking along the continental slopes[180,181] and the formation of North Atlantic Deep Water. This deep water is transported southwards in the Atlantic deep western boundary current and dispersive interior pathways[90]. The deep waters recirculate round the Southern Ocean and the rest of the global oceans, with the circulation being closed through wind-driven upwelling in the Southern Ocean[182] and mixing of dense waters globally.

Since currents in the Atlantic tend to transport upper waters northwards and deeper waters southwards, the circulation is often visualised in a two dimensional plane of latitude and depth or density, creating an "overturning streamfunction". The AMOC streamfunction (right hand face of Figure) is calculated by integrating the meridional (north-south) velocity across the Atlantic basin and cumulatively in depth. The strength at a given latitude is the maximum value in depth. The AMOC can also be calculated in density coordinates (where the northwards and southwards branches are defined in lighter and denser waters respectively) to better account for heat and buoyancy redistribution in the ocean. These two vertical coordinates give similar estimates of overturning in the subtropics where light waters overlay dense waters, but they differ at higher latitudes where the light inflow and dense outflow are found at similar depths[86].

ToC blurb

The Atlantic Meridional Overturning Circulation (AMOC) has a key role in the climate system. This Review documents AMOC variability since 1980, revealing periods of decadal-scale weakening and strengthening that differ between sub-polar and sub-tropical regions.

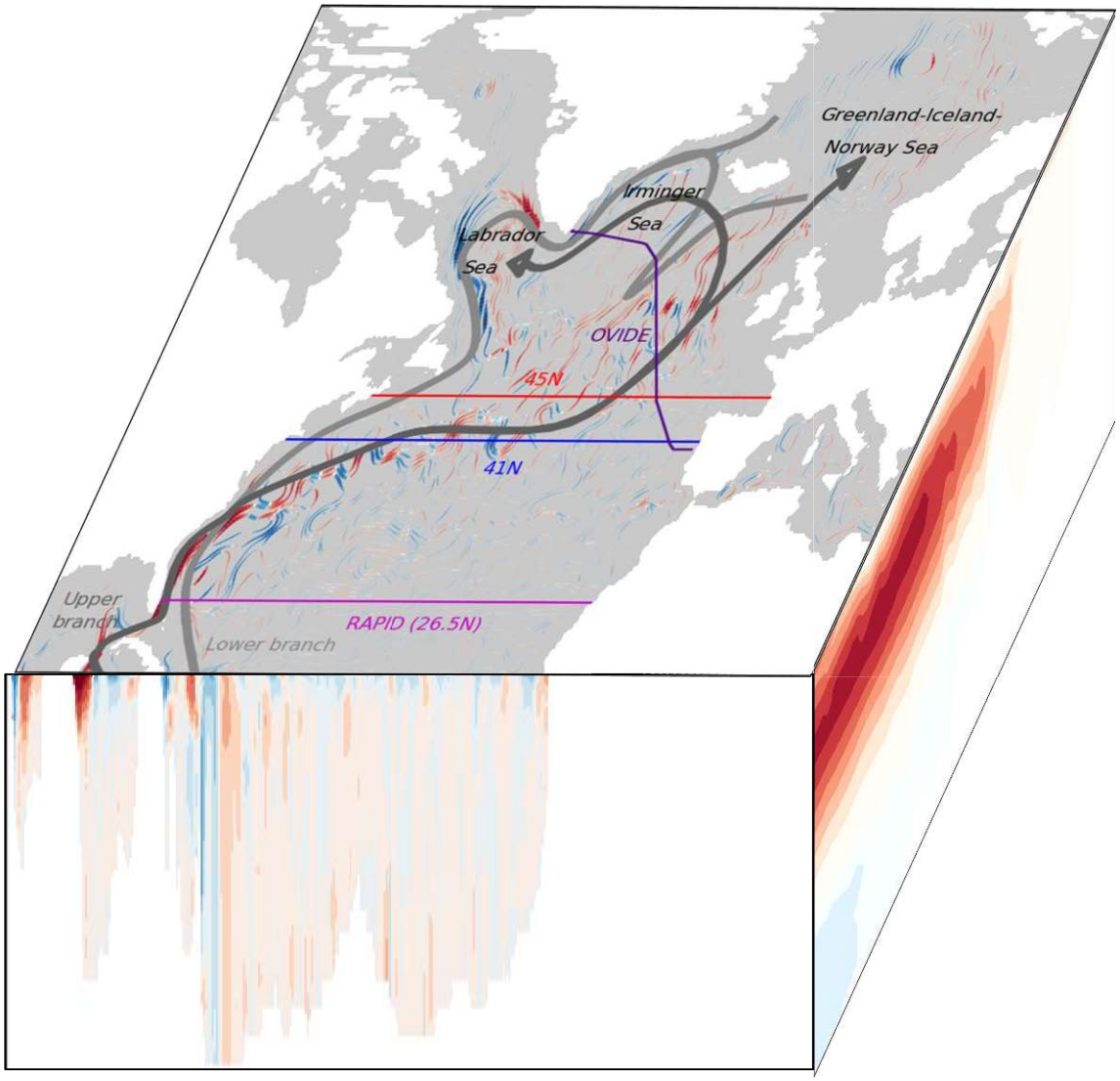
Greenland-Iceland-
Norway Sea
Irminger
Sea
Labrador
Sea
OVIDE
45N
41N
Upper
branch
RAPID (26.5N)
Lower branch